

CARBON ISOTOPE EFFECTS IN THE DECARBOXYLATION

OF

OXALOACETIC ACID

by

Alexander Wood, BSc.

A thesis presented in accordance with the regulations for
the degree of Doctor of Philosophy.

University of Glasgow.

December 1960.

ProQuest Number: 13850729

All rights reserved

INFORMATION TO ALL USERS

The quality of this reproduction is dependent upon the quality of the copy submitted.

In the unlikely event that the author did not send a complete manuscript and there are missing pages, these will be noted. Also, if material had to be removed, a note will indicate the deletion.



ProQuest 13850729

Published by ProQuest LLC (2019). Copyright of the Dissertation is held by the Author.

All rights reserved.

This work is protected against unauthorized copying under Title 17, United States Code
Microform Edition © ProQuest LLC.

ProQuest LLC.
789 East Eisenhower Parkway
P.O. Box 1346
Ann Arbor, MI 48106 – 1346

ACKNOWLEDGEMENTS.

The author wishes to express his thanks to Professor J.M. Robertson and Dr. E. Gelles as supervisors, to Dr. J. Waldron and Dr. S. Fitches of A.E.I. (Trafford Park, Manchester) for mass-spectrometric measurements, to Dr. R. Reed and Dr. J. Bell for their assistance with preliminary measurements and supply of isotopically enriched material in the C¹³ work and to Dr. S.J. Thomson for advice and the use of apparatus in the C¹⁴ work. The author was also in receipt of a grant from the Department of Scientific and Industrial Research.

Microanalyses were carried out by Mr. J.M.L. Cameron and the investigation reported on page 15 by Miss M. McNair, both of this department.

Contents.

	Pages.
<u>Summary.</u>	-
<u>General Introduction</u>	1-10.
1. Introduction	1-2.
2. Objectives	3.
3. Reaction System	3-4.
4. Previous Work	4-6.
5. Outline of Experimental Techniques and Calculations	6-10.
<u>The C¹³ Isotope Effect in the Decarboxylation of Oxaloacetic Acid</u>	11-30.
Part I : Studies with Oxaloacetic Acid of normal C ¹³ content	11-17.
A : Experimental	11-15.
Table of results	16.
B : Conclusion (interim)	17.
Part 2 : Studies with Oxaloacetic Acid en- riched in Oxaloacetic Acid-1-C ¹³	17-30.
A : Preparation	17-23.
B : Experimental and Results	23-24.
C : Conclusion (interim)	24-25.
D : Discussion of C ¹³ results	25-29.
1. Experimental Data	25-27.
2. Comparison with Theory	28.

3. Comparison with Literature Data ..	29.
Interim Conclusion on C ¹³ work	29-30.
<u>The C¹⁴ Isotope Effect in the Decarboxylation of</u>	
<u>Oxaloacetic Acid</u>	31-52.
Introduction	31.
Part 1 : Preparation of C ¹⁴ -enriched Oxalo-	
acetic Acid	32-33.
Part 2 : Apparatus	34-37.
Part 3 : Outline of Experimental Technique	
and Theory	37-39.
Part 4 : Experimental Procedure	40-44.
Example	42-44.
Part 5 : C ¹⁴ results	45-46.
Part 6 : Discussion of C ¹⁴ results	47-51.
1. Analysis	47-48.
2. Comparison with Theory	48-49.
3. Comparison with Literature Data	49-51.
Interim Conclusion on C ¹⁴ work	51-52.
<u>Analysis and Discussion of Carbon Isotope Effects</u>	
<u>in Decarboxylation</u>	53-80.
Part 1 : Experimental Results	53-59.
1. Results for Oxaloacetic Acid	53-54.
2. General Literature Survey of Carbon	
Isotope Effects in Decarboxylation .	55-59.
Part 2 : General Theoretical Section	60-66.

1. General Theory	60-63.
2. The Temperature-Independent Factor	64-66.
Part 3 : Application of Kinetic Isotope	
Effect Theory to Decarboxylations	66-74.
1. The Bigeleisen Approach	66-72.
2. Pitzer's Model	73-74.
Part 4 : The Paramagnetic Catalysis Theory .. 74-76.	
Part 5 : Final Summary and Conclusions	
Future Prospects	79-80.
<u>Appendices</u>	81-94.
<u>References</u>	95-97.

Figures.

	Page.
Fig. 1. Plot of kinetic isotope effect v. N_{X^0}/N_X for various f-values	9.
Fig. 2. Standard Reaction Vessel	11.
Fig. 3. Carbon Dioxide Purification Train for C ¹³ work	13.
Fig. 4. Mass-spectrometer Sample Tube	14.
Fig. 5. Plan of Synthesis of C ¹³ -enriched Oxaloacetic Acid	18.
Fig. 6. Apparatus for Synthesis of C ¹³ -enriched Acid	19.
Fig. 7. Apparatus for Synthesis of C ¹³ -enriched Acid	20.
Fig. 8. Plot of Experimental and Theoretical Isotope Effects v. 1/T ⁰ A	29.
Fig. 9. Vacuum Line for C ¹⁴ work	34.
Fig. 10. Gas Counter	35.
Fig. 11. Wiring of supplementary HT Batteries	37.
Fig. 12. Typical Counter Characteristic Curve	44.
Fig. 13. C ¹³ Kinetic Isotope Effect plotted against Temperature (Bigeleisen).....	72.
Fig. 14. C ¹⁴ Kinetic Isotope Effect plotted against Temperature (Bigeleisen).....	72.
Fig. 15. C ¹⁴ Kinetic Isotope Effect plotted	

- against Temperature (Pitzer)..... 73.
Fig. 16. C¹³ Kinetic Isotope Effect plotted
against Temperature (Pitzer)..... 74.

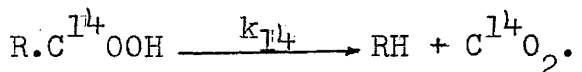
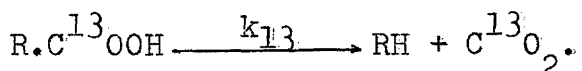
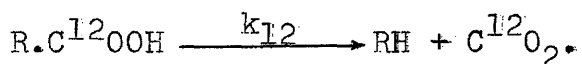
Tables.

	Page.
1. Decarboxylation Isotope Effects for ordinary Oxaloacetic Acid	16.
2. Decarboxylation Isotope Effects for C ¹³ -enriched Oxaloacetic Acid	24.
3. Summary of Experimental C ¹³ Isotope Effects for Decarboxylation of Oxaloacetic Acid	24.
4. Analysis of C ¹³ Results	27.
5. Results of C ¹⁴ Experiments	46.
6. Summary of C ¹⁴ Isotope Effects	45.
7. Analysis of C ¹⁴ Results	48.
8. Summary of Experimental and Theoretical C ¹⁴ Intermolecular Kinetic Isotope Effects	49.
9. Summary of Experimental Values of the Ratio (C ¹⁴ - I)/(C ¹³ - I)	50.
10. Summary of C ¹³ and C ¹⁴ Isotope Effects for Oxaloacetic Acid and Complexes	54.
11. Items in a Calculation of a Kinetic Isotope Effect	68.
12. Items in a Calculation of a Kinetic Isotope Effect	70.
13. Values of Isotope Effect v. N _{x0} /N _x for graph of Fig. 1	83.
14. Items in a Calculation of an Isotope Effect	94.

CARBON ISOTOPE EFFECTS IN THE DECARBOXYLATION OF OXALOACETIC ACID.

Summary.

Kinetic isotope effects in the decarboxylation of oxaloacetic acid were studied at 25° in aqueous solution for the acid alone, and then in turn in the presence of the cations of the rare earth metals yttrium, dysprosium and gadolinium, which act as catalysts through complex formation. Both acid and complexes decompose by known mechanisms with first order kinetics and at convenient rates. The three isotopes investigated were C¹², C¹³ and C¹⁴, and the reactions were,



The purpose of the work was to show the presence of an isotope effect (i.e., to show that the reaction rates decreased as the mass of the isotopic carbon increased), to investigate the effect of the catalytic metal ions and obtain values of the isotope effect for the various decarboxylating species, and to ascertain any possible effects due to the paramagnetic ions of dysprosium and gadolinium, in view of the known paramagnetism of C¹³, caused by its nuclear spin. Experimental results were also to be compared with theoret-

ically calculated isotope effects.

Ordinary carbon contains about 1% of C¹³, so ordinary oxaloacetic acid can be used to determine the first isotope effect, i.e., the ratio k_{12}/k_{13} . This was done by analysing the purified effluent carbon dioxide from the reaction, at various fixed stages of completeness, by means of a mass spectrometer. The reaction involving the heavy isotope is a little slower than the light one, so the carbon dioxide appears to have an abnormally low C¹³ content and from this k_{12}/k_{13} can be calculated.

The experiments were repeated using oxaloacetic acid enriched in oxaloacetic acid-1-C¹³ to about 4%, in order to facilitate the mass-spectrometric measurements. This enriched material was prepared from enriched barium carbonate via a Grignard reaction, giving enriched sodium acetate. The salt was converted into ethyl acetate and thence diethyloxaloacetate obtained by means of a Claisen condensation with diethyl oxalate. The enriched acid was obtained in a satisfactory state of purity by acid hydrolysis of the diethyl ester. Isotope effects similar to those already observed for ordinary oxaloacetic acid were found on repeating the experiments with the enriched material.

The k_{12}/k_{14} ratios were obtained using oxaloacetic acid enriched in oxaloacetic acid-1-C¹⁴. The preparation was the same as before, but started from labelled sodium acetate.

Since C^{14} is β -radioactive, the samples of effluent carbon dioxide were analysed by counting measured volumes in a Geiger counter, using a simple standard technique, k_{12}/k_{14} being derived in a manner similar to that used for k_{12}/k_{13} .

The results of the work showed the presence of definite isotope effects and these are summarised below :

Reaction	Uncatalysed	YA^+	$DyA^+(p)$	$GdA^+(n)$
k_{12}/k_{13}	1.046	1.037	1.036	1.039
k_{12}/k_{14}	1.132	1.108	1.106	1.113

Under the reaction conditions the most important species in the catalysed reactions are the complexes shown between the metal ions and the dianion A^{2-} of oxaloacetic acid. (n) indicates the paramagnetic ions.

The theoretical values for k_{12}/k_{13} and k_{12}/k_{14} are 1.044 and 1.083 respectively at 25° . The similarity between the results in each row for the complexes is ascribed to the similar nature of the metal ions in the complexes and gives no indication of any paramagnetic effect. The difference between the kinetic isotope effect for the uncatalysed reaction and the corresponding effect for the complexes is attributed to the inductive effect of the metal ions. It was observed that the theoretical approach gave a fairly satisfactory value for k_{12}/k_{13} , but a less satisfactory result for k_{12}/k_{14} .

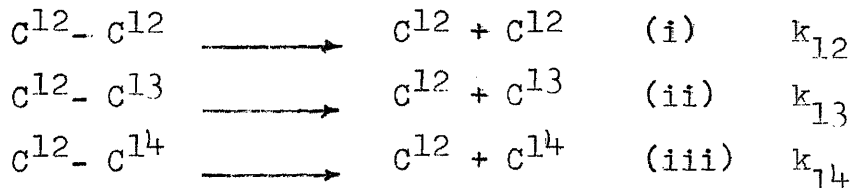
CARBON ISOTOPE EFFECTS IN THE DECARBOXYLATION OF
OXALOACETIC ACID.

1. INTRODUCTION.

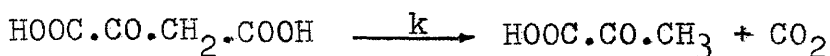
The term 'isotope effect' refers to the fact that under certain conditions in a chemical reaction one isotope of an element can react at a slightly different rate from another. For quite some time after the recognition of the existence of isotopes it was generally considered that the isotopes of any given element were identical chemically, in spite of their differences in masses or radioactive properties. However, after the separation of the hydrogen isotopes in 1932-3, and the study of their properties in exchange reactions, small variations in equilibrium constants were found between the several isotopic species. Similar effects were also shown both theoretically and experimentally (8) to be present, though to a lesser extent, among isotopes of heavier elements. These early investigations were of special importance in the preparation of isotopically enriched materials. Most of the early work, apart from studies of hydrogen isotopes, concerned exchange equilibria, and it was not until after the war that kinetic studies of isotopic rates of reactions were developed. The concept of the kinetic isotope effect has particular application in the study of reaction mechanisms, since a

kinetic isotope effect will only be observable if the rate determining step involves reaction at the isotopic centre. This is because the rate of reaction of the heavier isotope generally tends to be less than that of the lighter one and this effect will only appear if the difference in rates can be reflected in the net rate equation. In fact, most experiments involving the use of isotopes, e.g., as tracers, are open to error on this account if possible kinetic isotope effects are overlooked. Kinetic isotope effects can also be examined as a problem in their own right, and in the present study, the field chosen was the study of the effects for isotopes of carbon, C¹², C¹³, and C¹⁴.

To do this, a set of reactions involving the following bond fissions



were chosen and their relative rates determined as explained below. In practice, the problem was referred to a decarboxylation reaction, the decarboxylation of oxaloacetic acid, HOOC.CO.CH₂.COOH,



The isotopically labeled atom is starred. k is the rate constant.

2. OBJECTIVES.

There were four main objectives in this work. Firstly, it was necessary to show that the above reaction did, in fact, give a kinetic isotope effect; i.e., that the rates of the three reactions given on page two were in the order (i) > (ii) > (iii). Secondly since the reaction is catalysed by metal ions of the transition series, which act via complex formation, the effect of these ions was to be investigated and the isotope effects for the various decarboxylating species obtained and inter-compared. In particular, it was desired to ascertain any possible effects due to paramagnetic ions, in view of the known paramagnetism of C¹³, caused by its nuclear spin. Finally, experimental results were to be compared with theoretically calculated kinetic isotope effects.

3. REACTION SYSTEM.

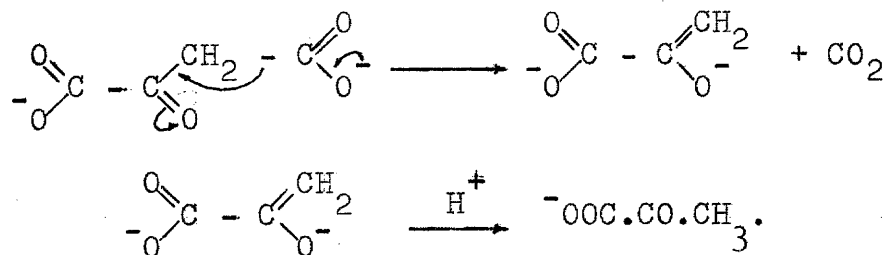
The choice of the decarboxylation of oxalic acid as a reaction system was dictated by the following considerations. Firstly, the isotopes concerned are those of one of the most important elements, namely, carbon. Also, since ordinary carbon already contains about 1% C¹³, the first pair of reactions above (i) and (ii) may be studied using unenriched material. The selection of decarboxylation is mainly on the grounds that the reaction is

usually first order and this simplifies the theoretical work (in particular, the so-called C¹³ kinetic isotope effect, e.g., is simply measured by the ratio k_{12}/k_{13}), but more especially in that the reaction, by evolving carbon dioxide, lends itself readily to the determination of relative rates of isotopically competitive reactions. This is done by noting that since the heavy isotope's reaction rate is less than that of the light isotope, the concentration of heavy isotope in the effluent carbon dioxide appears to be abnormally low at first and this drop in heavy isotope content can be interpreted in terms of the relative rates of the two parallel reactions. Oxaloacetic acid was very suitable since it decarboxylates at a convenient rate in water at 25° by a first order process and also can complex with transition metal ions, which act as catalysts. Rare earth ions were particularly useful in the latter respect, the ions chosen being those of gadolinium (Gd; paramagnetic), yttrium (Y; diamagnetic) and dysprosium (Dy; paramagnetic), these last two having the same charge, ionic radius and similar association constants with oxaloacetic acid.

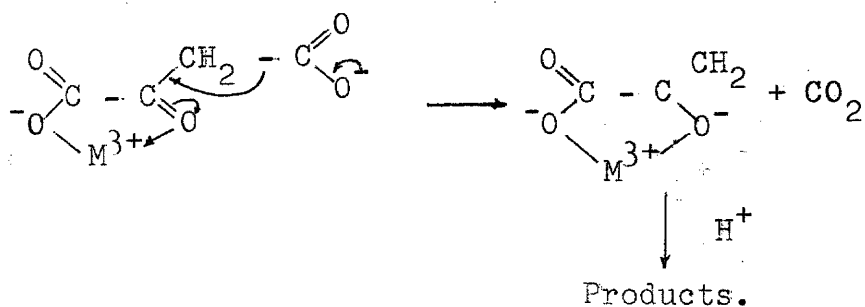
4. PREVIOUS WORK.

Only previous work insofar as it relates to the subject of this thesis will be noted for the moment. Some

support for a paramagnetic catalysis effect had been obtained by the observation by Pitzer and co-workers that paramagnetic ions can catalyse decarboxylations to an extent beyond that inferable from a comparison between these ions and others of similar size, charge and association constants (4, 5, 6). Rare earth metal ions were particularly useful in this respect. Further amplification of this work came in papers by Gelles on oxaloacetic acid (2, 7, 8 and 9) and the kinetics and mechanism of the decarboxylation of oxaloacetic acid alone, and in the presence of these ions were investigated (8, 9, 10). The mechanism of the reaction is,



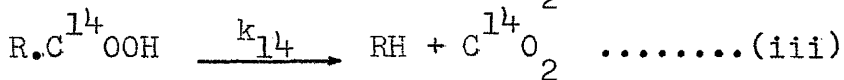
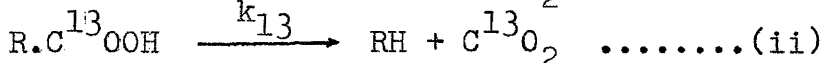
For the metal-ion catalysed reaction, where the chief complex is of the form MA^+ (8), where M is the trivalent rare earth cation and A^{2-} the dianion of oxaloacetic acid, we have,



It was thought, for reasons to be discussed later in more detail, that the presence of paramagnetic ions would cause the corresponding C¹³ kinetic isotope effects to be unusually high, i.e., e.g., the k₁₂/k₁₃ value for the dysprosium (paramagnetic) catalysed reaction would be larger than the value for the yttrium (diamagnetic) catalysed one and this in turn would be approximately equal to the k₁₂/k₁₃ for the uncatalysed reaction. Preliminary investigations (11) seemed to substantiate this hypothesis. The C¹⁴ effects were supposed to be unaffected paramagnetically.

5. OUTLINE OF EXPERIMENTAL TECHNIQUES AND CALCULATIONS.

For all three of the isotopically competitive reactions we have the first order processes:



where R.COOH represents oxaloacetic acid. The ks are the first order rate constants.

Ordinary carbon contains about 1.1% C¹³ and a negligible amount of (radioactive) C¹⁴. Hence although reactions (i) and (ii) may be studied without needing to prepare oxaloacetic acid enriched in oxaloacetic acid-C¹³, the pair (i) and (iii) can only be investigated using specially prepared material. Note that the group R in the

equations is assumed to be all-C¹² (so we studied the relative rates for the fission of the bonds C¹² - C¹², C¹² - C¹³ and C¹² - C¹⁴); since the natural abundances of C¹³ and C¹⁴ are low, this is a good approximation. Further, the reactions were studied in pairs to obtain the isotope effects: it would be difficult to study the rates absolutely in turn and obtain accurate intercomparisons; also the cost of preparing the pure 1-C¹³ and 1-C¹⁴ oxaloacetic acids would be practically prohibitive. The method of analysis for both pairs of reactions was to find the isotopic content of the effluent carbon dioxide after a known degree of reaction.

Each pair was treated separately. For the 'C¹³' ratio, k_{12}/k_{13} , the analyses were performed using a mass spectrometer to find the ratio C¹³O₂ / C¹²O₂. In the C¹⁴ work the value of C¹⁴O₂ / C¹²O₂ was measured at similar stages, but using a Geiger counter to estimate the C¹⁴O₂ content.

To calculate the ratio k_{12}/k_{13} , say, the formula,

$$\frac{k_{12}}{k_{13}} = \frac{\log_{10} \left(1 - f(N_{x^0} + 1) / (N_x + 1) \right)}{\log_{10} \left(1 - f N_x (N_{x^0} + 1) / N_{x^0} + 1 \right)} \dots \text{(iv).}$$

was used. $N_x = C^{13}O_2 / C^{12}O_2$ at time t, N_{x^0} is the isotope ratio at infinite time and f is the overall fraction of reaction. The formula may be readily obtained from the simple first order equation,

$$kt = \ln a / (a - x).$$

Here, for the C^{13} work, e.g., we have,

$$k_{12} t = \ln a_{12} / (a_{12} - x_{12}) = - \ln (1 - x_{12}/a_{12}).$$

A similar expression can be written for k_{13} .

$$\therefore \frac{k_{12}}{k_{13}} = \frac{\ln (1 - x_{12}/a_{12})}{\ln (1 - x_{13}/a_{13})} \dots \dots \dots \text{(v)}.$$

Now,

$$N_x = [C^{13}O_2] / [C^{12}O_2] = x_{13}/x_{12} \text{ at time } t,$$

$$N_{x^o} = " = a_{13}/a_{12} "$$

and f = overall completeness of reaction

$$= (x_{12} + x_{13}) / (a_{12} + a_{13}).$$

$$\therefore f = \frac{x_{12} + x_{12} \cdot N_x}{a_{12} + a_{12} \cdot N_{x^o}} = \frac{x_{12}(1 + N_x)}{a_{12}(1 + N_{x^o})}.$$

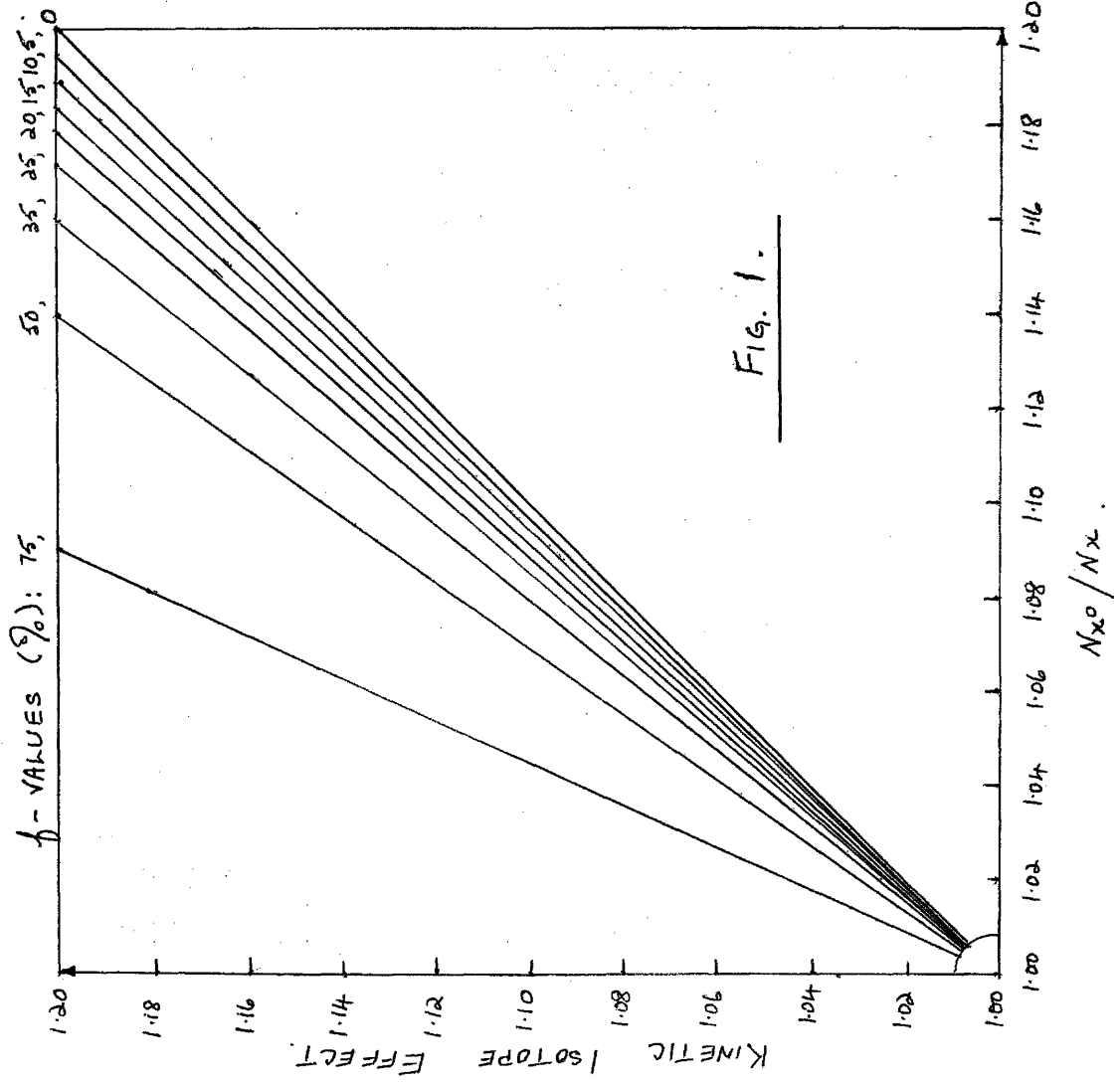
$$\therefore x_{12}/a_{12} = f(N_{x^o} + 1) / (N_x + 1).$$

Similarly,

$$x_{13}/a_{13} = fN_x(N_{x^o} + 1) / N_{x^o}(N_x + 1).$$

Substitution of the expressions for x_{12}/a_{12} and x_{13}/a_{13} in equation (v), and changing the base of the logs. from e to 10, gives equation (iv).

It is usually desirable to make measurements of



N_x at relatively low f-values (up to 50% at most), since the error in determining k_{12}/k_{13} , e.g., varies with f, increasing as f increases. This is discussed more fully by Bigeleisen and Allen (12) and also in appendix A. When the isotopic ratio N_{x0} is small and/or k_{12}/k_{13} is practically unity (as in fact it is here), $(N_{x0} + 1)$ becomes very nearly equal to $(N_x + 1)$, so,

$$\frac{k_{12}}{k_{13}} = \frac{\log(1 - f)}{\log(1 - fN_x/N_{x0})}$$

or, $(1 - fN_x/N_{x0})^{k_{12}/k_{13}} = (1 - f).$

This is the formula given by Bothner-By and Bigeleisen (13). To work out the values of k_{12}/k_{13} , e.g., from the N_x/N_{x0} data for the various given values of f, a convenient calculating graph was drawn. A facsimile is shown in Fig. 1 and data for the graph are given in appendix B. The f-contour lines are almost straight, very slight curvature appearing only above 75%, even on the large-scale graph used to handle the results. Errors in the kinetic isotope effect due to errors in N_{x0}/N_x and/or f can be readily estimated from the curve. For enriched isotopes, the graph gives only approximate results.

The procedure for both C^{13} and C^{14} work was to drop a little glass bucket containing some oxaloacetic acid into a given degassed solution in an evacuated vessel,

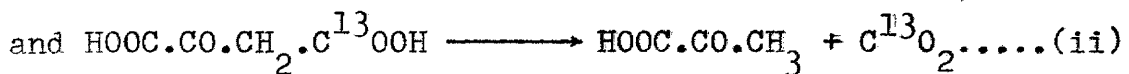
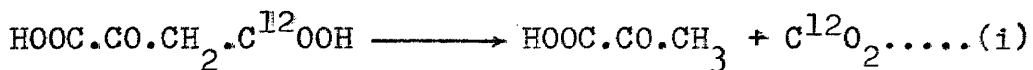
let the reaction run, in a thermostat, to a predetermined degree of completeness, as calculated from the data by Gelles and Clayton (8), stop the reaction by chilling the apparatus in acetone/Drikold and analyse the effluent carbon dioxide. For the C¹³ work, the carbon dioxide was purified by several sublimations from acetone/Drikold to liquid air, along a vacuum line, and finally trapped in a mass spectrometer sample tube. The tube was sealed off and sent for analysis. For the C¹⁴ work, the radioactive carbon dioxide was sublimed two or three times and then the amount carefully measured in a Macleod Gauge. This carbon dioxide was then mixed with diluent carbon dioxide and carbon disulphide by a simple standard technique and the mixture passed into a Geiger tube for counting. In both cases, the isotopic content was determined and thence the kinetic isotope effect, as noted above.

The work done will now be discussed, taking the C¹³ work first. This latter is in two parts, firstly the study of ordinary oxaloacetic acid and secondly the study of oxaloacetic acid enriched in oxaloacetic acid-1-C¹³.

The C¹³ Isotope Effect in the Decarboxylation
of Oxaloacetic Acid.

Part 1 : Studies with oxaloacetic acid containing only the normal C¹³ content.

A. The reactions are,



Because of the low C¹³ content of normal carbon, all the C¹²O₂ can be taken to come from C¹²-C¹² bond fission and all the C¹³O₂ from C¹²-C¹³ bond fission.

A suitable reaction vessel was designed (Fig. 2),

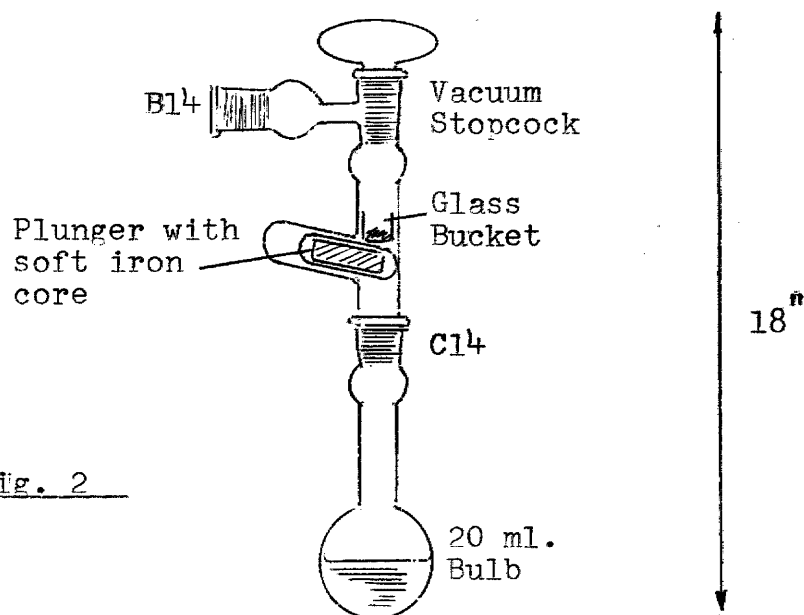
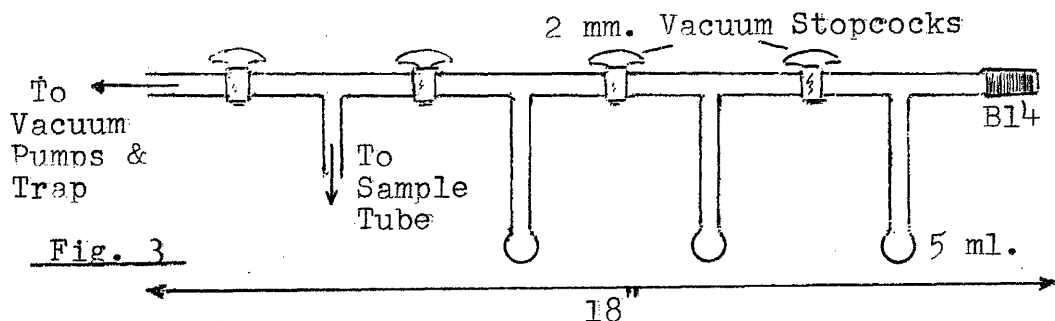


Fig. 2

and 250 ml. solutions of yttrium, dysprosium and gadolinium chlorides (hereafter referred to as Y^{3+} , etc.) and KCl made up as explained in Gelles and Clayton's paper (8), but with the modification that, after weighing out the rare earth oxide directly into the graduated flask, 100 ml. of 0.4N HCl (made up from four B.D.H. ampoules in 500 ml.) was added. After the oxide had dissolved, each solution was made up to the mark with distilled water and checked by titration, adding first a little saturated potassium oxalate solution (about $\frac{1}{2}$ ml., say) to precipitate the rare earth ions. These ions were each 0.2M and had (excess) $[\text{H}^+]$ of 0.1N. The KCl was 0.12M KCl and 0.10N HCl. Hence the ionic strength of each solution was 0.22.

A 10 ml. sample of Y^{3+} , e.g., was pipetted into the reaction vessel's bulb and the glass bucket containing 0.0264 gm. of oxaloacetic acid (making the acid 0.02M) slipped in and rested on the plunger. The bulb was chilled in acetone/Drikold, the vessel evacuated, using a rotary pump and a mercury diffusion pump with a liquid air trap, then allowed to warm up to room temperature, rechilled and repumped once or twice more to ensure efficient degassing. The side arm was then stoppered and the whole immersed in a thermostat at $25^\circ \pm 0.01$. After a quarter of an hour, the reaction was started by pulling back the plunger, using a strong magnet, so that the bucket fell into the solution.

The flask was swirled in the tank until the oxaloacetic acid had dissolved and the reaction allowed to run to a definite completeness (e.g., 10%), using a stopwatch to measure the time, calculated from Gelles & Clayton's data (8). The bulb was then chilled suddenly, with swirling, in acetone/Drikold and the vessel connected to the purification train shown in Fig.3.



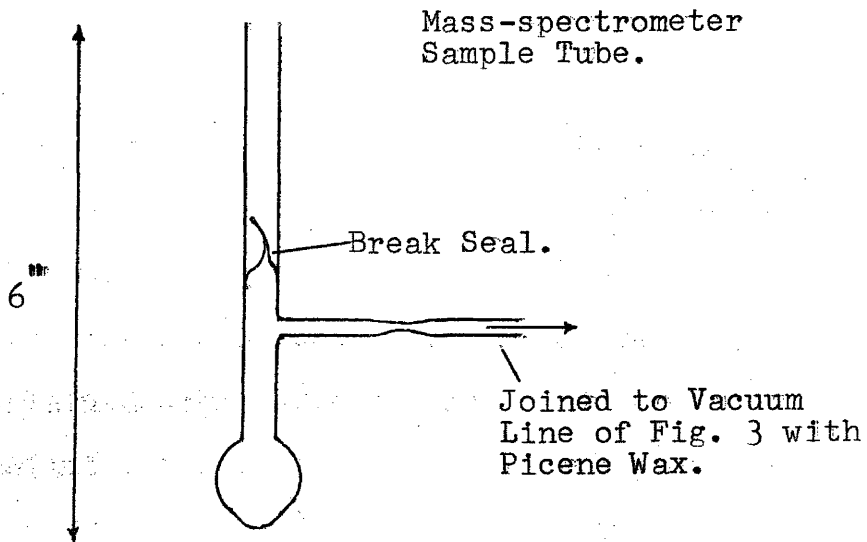
(Note that the lead to the mass-spectrometer sample tube is really at right angles to the plane of the paper.)

The carbon dioxide was sublimed through the train from one bulb (in acetone/Drikold) to another (in liquid air), finally ending up in the sample tube (see Fig.4). This was sealed off and the contents presently analysed.

Several different types of reaction vessel were tried in the extensive preliminary experiments, the one shown in Fig.2 proving to be the most convenient. There were considerable difficulties with the mass-spectrometric analyses: the 45/44 peak height ratios were found at first to be much too high, due to some impurity. A considerable

improvement was obtained after the introduction of the

Fig. 4



purification train and solution degassing. Apart from some preliminary work, the analyses were all done by Metropolitan-Vickers Ltd. (now AEI) on MS-2 machines, using the double inlet technique, whereby the observed 45/44 peak height ratio for a given sample is compared quickly with the 45/44 ratio for standard tank carbon dioxide. This was done several times for each sample and the N_x (or N_x^o , as the case may be) for each sample corrected by comparing the corresponding value for the tank carbon dioxide with the true

accepted ratio for carbon dioxide, given by M-V as 1.112 \pm 0.002%. The 45/44 peak height ratios must then be corrected for O^{17} (due to $C^{12}O^{16}O^{17} = 45$) and resolution of the spectrometer and are then ready for use in calculating kinetic isotope effects. The following table gives a set of data which were considered accurate.

The O^{17} correction was done by subtracting 0.075 from the observed peak height ratio. The N_x^o values, i.e., the (45/44) values for the infinity reaction, were measured from reaction carbon dioxide: each set of tubes sent for analysis contained some infinity runs. Since the results for these infinity analyses varied a little from set to set, each sets N_x^o 's are compared with its own mean N_x^o . Each reaction solution was degassed at least once (the effect of atmospheric carbon dioxide on the analyses can readily be shown to be much less for the unenriched case than for the enriched). It was found that the rate constant given for the uncatalysed reaction was in error: a redetermination, using the technique described by Gelles, Pitzer & Hay gave a specific rate constant of 0.217×10^{-3} . Hence the true f-values are about one third of those calculated initially. The errors quoted in Table 1 are standard deviations.

Table 1.

No.	Run	$N_x =$ (45/44)	Carr.	N_x^O	N_x^O/N_x	KIE	
1	10%Y ³⁺	1.094	1.126	1.029	1.031		
2	15%Y ³⁺	1.091	1.126	1.032	1.035	Mean = 4.151/4	
3	15%Y ³⁺	1.085	1.123	1.035	1.038	= 1.038 ± 0.006	
4	20%Y ³⁺	1.090	1.136	1.042	1.047		
5	10%Dy ³⁺	1.085	1.123	1.035	1.037		
6	15%Dy ³⁺	1.087	1.123	1.033	1.036	Mean=4.170/4 =	
7	20%Dy ³⁺	1.086	1.136	1.046	1.052	1.043 ± 0.007	
8	25%Dy ³⁺	1.093	1.136	1.039	1.045		
9	10%Gd ³⁺	1.090	1.123	1.030	1.032		
10	15%Gd ³⁺	1.092	1.126	1.031	1.034	Mean=4.159/4	
11	20%Gd ³⁺	1.090	1.136	1.042	1.047	= 1.040 ± 0.007	
12	25%Gd ³⁺	1.092	1.136	1.040	1.046		
13	3.3%KCl	1.080	1.123	1.040	1.041		
14	5.0%KCl	1.086	1.126	1.037	1.038	Mean=4.187/4	
15	6.8%KCl	1.080	1.136	1.052	1.054	= 1.047 ± 0.007	
16	8.7%KCl	1.080	1.136	1.052	1.054		

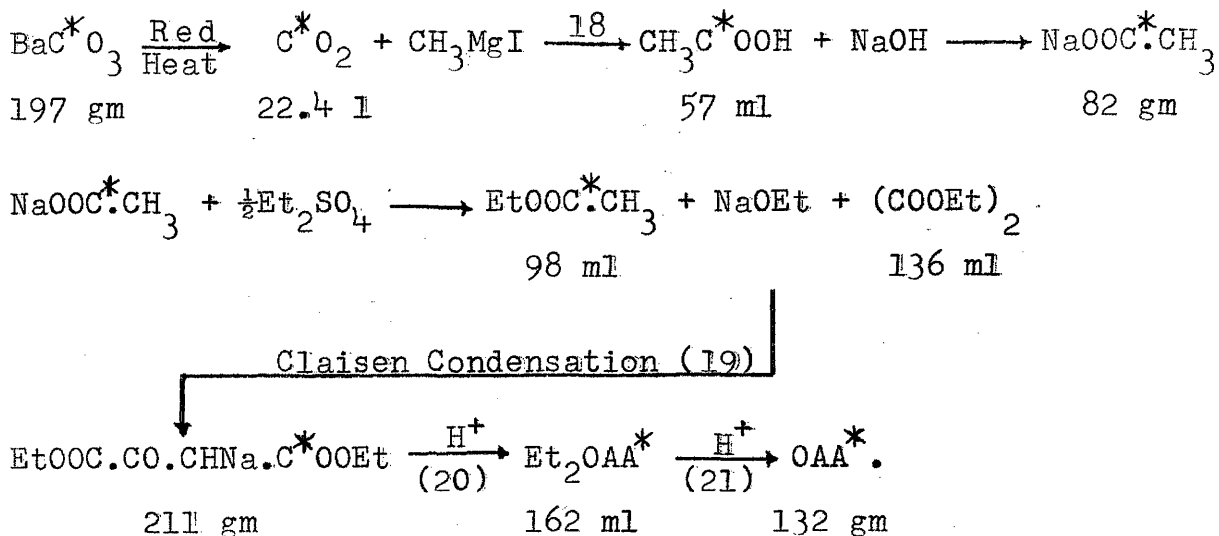
KIE = Kinetic Isotope Effect.

B. Conclusion to Part 1.

It can be observed from the table that the catalysed reactions all give about the same kinetic isotope effect, whereas the uncatalysed reaction has a slightly higher kinetic isotope effect. Due to the low C¹³ content of ordinary carbon, however, it was desired to improve the accuracy of the mass spectrometric measurements by preparing oxaloacetic acid enriched in oxaloacetic acid-l-C¹³ and studying its decarboxylation.

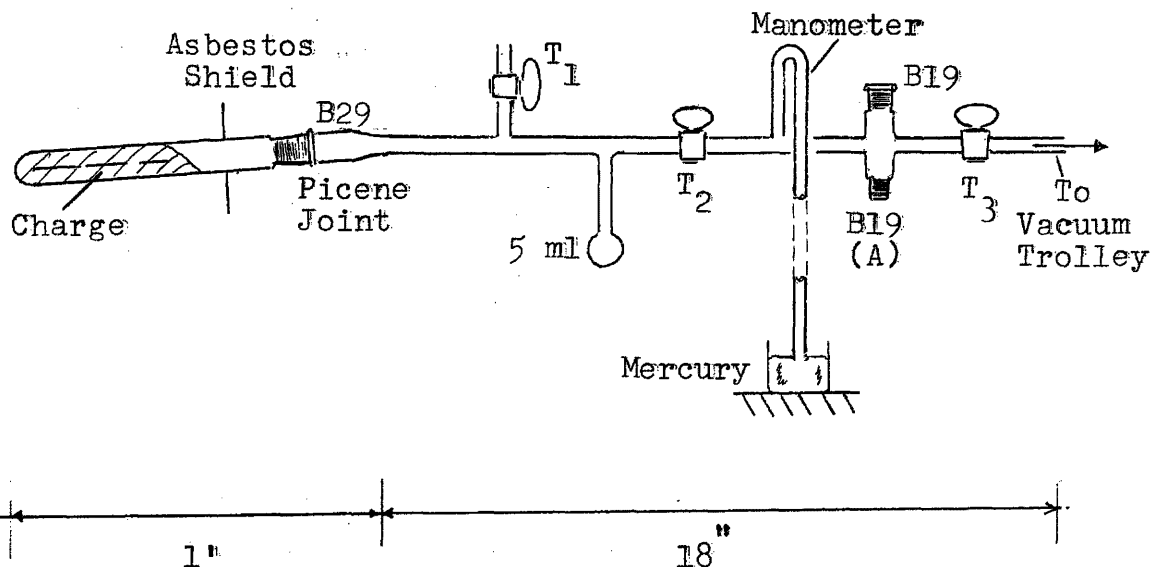
Part 2 : Studies of C¹³ kinetic isotope effects using
oxaloacetic acid enriched in oxaloacetic acid-l-C¹³.

A. The first problem was the preparation. The method is outlined in Fig.5 and the apparatus used shown in Fig.6. The method followed was a convenient modification of the methods discussed by Yankwich et al. (17). Before doing the synthesis with the enriched carbonate, each step was checked at least twice. The charge was 0.52 gm. enriched carbonate, 5.46 gm. ordinary carbonate and 60 gm. washed and dried lead chloride, all ground and mixed together carefully. The apparatus was evacuated, T₃ closed and the furnace switched on. The heating was continued for two hours in all. While the decomposition was in progress and the enriched

Fig. 5.

Notes:-

- a) Et_2OAA and OAA represent diethyl oxaloacetate and oxaloacetic acid respectively.
- b) About $7\frac{1}{2}\%$ C^{13} enrichment budgeted for. The enriched carbonate contained 1 gm. C^{13} in 20.30 gm. carbonate. (See Appendix C).
- c) The quantities of methyl iodide, magnesium and diethyl sulphate used were four times the stoichiometric amounts.
- d) 4 gm. oxaloacetic acid planned for.
- e) The barium carbonate used was mixed with ten times its weight of lead chloride, a flux.

Fig. 6 (Not to scale)

Notes:-

- a) 3 mm. vacuum taps and $\frac{1}{4}$ " tubing used.
- b) Manometer 80 cm. from mercury level in cistern to top.
- c) Charge in furnace had a hole poked down the middle to permit easy egress of gas on heating.
- d) Furnace tube heated by a small electric furnace, controlled by a calibrated rheostat.

carbon dioxide condensing in the 5 ml. bulb, cooled in liquid air, the Grignard reagent was prepared in the apparatus of Fig. 7 from 3 gm. magnesium, 7.5 ml. methyl iodide (dried over anhydrous calcium sulphate), 100 ml. dry ether

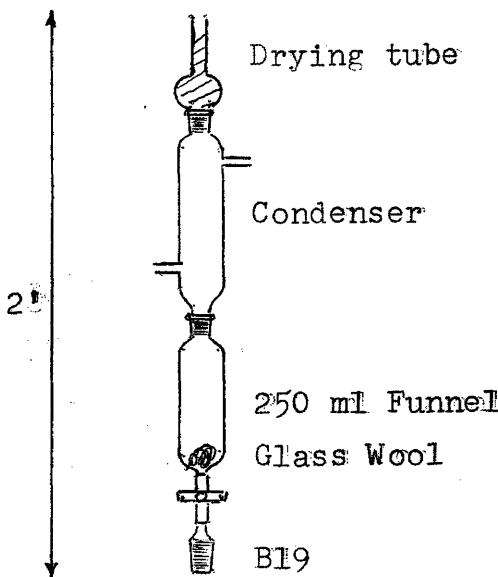


Fig. 7. The glass wool is to trap any unreacted magnesium.

and a small crystal of iodine. The reaction was started by warming the apparatus a little with a hairdryer. The furnace was then switched off and the Grignard solution run smoothly from the apparatus of Fig. 7 into a 250 ml. RB flask connected at A (Fig. 6). The Grignard apparatus was rinsed down with more ether, removed and the vacuum line, restoppered.

The solution was frozen in liquid air, the apparatus re-evacuated, T_3 closed and the enriched carbon dioxide transferred from the 5 ml. bulb (in acetone/Drikold) to the 250 ml. flask, allowing 10 minutes transfer time. With T_2 closed, the furnace was detached and the 250 ml. flask allowed to warm up to room temperature, with occasional shaking by rocking the apparatus to and fro a little. The mercury in the manometer went down by about the normal vapour pressure of ether at room temperature. The flask's contents were then poured into a beaker, slowly acidified to litmus with dilute sulphuric acid and extracted with 250 ml. ether in five portions. The extract was neutralised to litmus with dilute sodium hydroxide and the aqueous layer separated and carefully evaporated down to dryness. The yield was usually 90% or over.

The anhydrous sodium acetate produced was then refluxed with 8 ml. of vacuum redistilled diethyl sulphate for an hour, the ethyl acetate formed carefully fractionated and the liquid coming over at about 70° collected. The fractionation was carried out using a one-piece flask, vacuum-jacketed fractionating column and condenser unit. The loading of the flask was done via a B 10 side arm. The refluxing was performed in the same unit by tilting it so that the condenser acted as a simple reflux. This saved transfer losses, since the sodium sulphate produced caked. The yield

was nearly theoretical.

About 0.7 gm. sodium were atomised (69) and transferred with about 50 ml. sodium-dried ether to a 100 ml. flask fitted with a condenser and drying tube. Using a new piece of sodium gave very little oxide and most of what was present was easily washed away in the rinsing following atomisation. 2 ml. of superdry ethanol (70%) were added down the condenser, using a syringe, and the mixture left refluxing gently overnight on a mantle. The liquid should remain water-white. The condenser was then removed and an adaptor carrying a tap funnel and the condenser quickly put in its place. 4 ml. of dried $(COOEt)_2$ were then added, the flask chilled in ice and the enriched ethyl acetate run in drop by drop over twenty to thirty minutes, with swirling. Finally the mixture was refluxed for two hours.

The contents of the flask were then poured into a beaker, some water added and the mixture cautiously acidified to litmus with dilute sulphuric acid, with vigorous stirring. The diethyloxaloacetate produced was extracted with 250 ml. ether, the extract dried with anhydrous magnesium sulphate, most of the ether evaporated off and the diester carefully vacuum distilled, using the apparatus used previously for the ethyl acetate. Two main clear-cut fractions were obtained, the first (small) probably mainly $(COOEt)_2$ and the second, the diethyl oxaloacetate. The pump was run at full speed

and an applicator used to prevent bumping. The distillate was water-white and in about 50% overall yield from the barium carbonate. 3 ml. of concentrated hydrochloric acid and 3 ml. of glacial acetic acid were added to the diester fraction and the mixture left for three days in a small flask. About half the liquid was then evaporated off in vacuo, taking care not to heat the material to more than 40°, when the flask's contents solidified on cooling to room temperature. The flask was chilled in acetone/Drikold, and the contents presently dissolved in acetone, the solution filtered, warmed to concentrate it a little, some benzene added, and the whole left to crystallise. The yield of oxaloacetic acid was not above 50% as a rule. The purity was checked by infra-red analysis, titration (the observed equivalent was 66.4, compared with an ideal value of 66.0), microanalysis and by doing a manometric run (as described for the redetermination of the uncatalysed (KCl) decarboxylation rate) and was found satisfactory.

B. Experimental Results.

The experimental runs were performed as described before, but the initial solutions were degassed more than once, since the enriched-C¹³ results are sensitive to the presence of atmospheric carbon dioxide. The results are shown in Table 2 and are corrected for O¹⁷ and mass-spectrometric resolution errors.

	$N_x = 45/44$	N_x^0/N_x	KIE	Mean
1	20% Y	377.4 ± 0.5	1.032	1.036
2	25% Y	365.1 ± 0.4	1.067	1.078
3	20% Dy	377.8 ± 0.8	1.031	1.035
4	25% Dy	378.5 ± 0.5	1.029	1.033
5	20% Gd	376.7 ± 0.8	1.034	1.038
6	25% Gd	378.4 ± 0.8	1.030	1.034
7	6.8% HCl	373.1 ± 1.6	1.044	1.046
8	8.7% KCl	373.7 ± 1.5	1.043	1.045
9	∞	389.6	-	-

The infinity value is the mean of four infinity runs. The 25% Y run is clearly in error, being too high. The kinetic isotope effects were calculated using the equation on p. 9; f was taken as equal to f-overall for the unenriched decarboxylation.

C. Conclusion.

The results compare fairly well with those for unenriched oxaloacetic acid (p.16). A complete table (No.3) is given below.

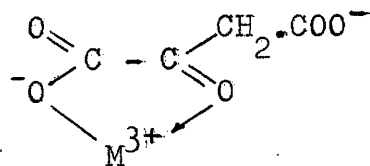
Table 3

Catalyst	Kinetic isotope effect
Y	1.037 ± 0.005
Dy	1.037 ± 0.007
Gd	1.039 ± 0.006
None (KCl)	1.046 ± 0.006

The errors are standard deviations; the 20% Dy³⁺ value (p. 16) has been omitted, as being rather high. The KCl value is marginally higher than the rest, and these are all practically identical, within the limits of experimental error.

D. Discussion of C¹³ results.

- If we assume (8) that the most important species contributing to the observed first order rate in the decarboxylation of oxaloacetic acid are the undissociated acid H₂A, the monoanion HA⁻, the dianion A²⁻ and the complex MA⁺, of the following structure,



we have,

$$\begin{aligned} \frac{d[\text{CO}_2]}{dt} &= k_{\text{obs}} [\text{H}_2\text{A}]_{\text{tot}} \\ &= k_0 [\text{H}_2\text{A}] + k_1 [\text{HA}^-] + k_2 [\text{A}^{2-}] + k_c [\text{MA}^+] \dots (i). \end{aligned}$$

If K₁, κ₁ and κ₂ are the thermodynamic dissociation and ionisation constants for MA⁺, H₂A and HA⁻, it can readily be shown that,

$$\frac{[\text{H}_2\text{A}]_{\text{tot}}}{[\text{H}_2\text{A}]} = \frac{[\text{H}_2\text{A}] + [\text{HA}^-] + [\text{A}^{2-}] + [\text{MA}^+]}{[\text{H}_2\text{A}]}$$

$$= \frac{1 + \frac{K_1}{f_1^2 [\text{H}^+]} + \frac{K_1 K_2}{f_1^2 f_2 [\text{H}^+]^2} + \frac{K_1 K_3 f_3}{f_1^2 [\text{H}^+]}}{1 + \frac{K_1}{f_1^2 [\text{H}^+]} + \frac{K_1 K_2}{f_1^2 f_2 [\text{H}^+]^2} + \frac{K_1 K_3 f_3}{f_1^2 [\text{H}^+]}}.$$

On inserting values for K_1 , K_2 , f_1 , f_2 , $[\text{H}^+]$ and an approximate (maximum) value for $[\text{M}^{3+}]$ of 0.02M, it can be shown that $[\text{H}_2\text{A}]_{\text{tot}} = [\text{H}_2\text{A}]$. The K s and K_1 were obtained from references 2 and 23, the activity coefficients calculated from the Davies Equation (2) and the pH gives $\{\text{H}^+\}$. The pH was measured and found to be 1.02 over the larger part of the reaction.

$$\therefore k_{\text{obs}} = k_0 + \frac{k_1 [\text{HA}^-]}{[\text{H}_2\text{A}]} + \frac{k_2 [\text{A}^{2-}]}{[\text{H}_2\text{A}]} + \frac{k_c K_1 K_2 [\text{M}^{3+}]}{\{\text{H}^+\}^2} \cdot \frac{f_3}{f_1} \dots (\text{ii})$$

This is the equation given by Gelles and Clayton (8). Since K_1 , K_2 and k_c refer respectively to the dissociation of MA^+ , H_2A and HA^- , and these processes do not directly involve the isotopic carbon atom, they can be taken to be practically invariant with respect to isotopic substitution, the maximum size of any secondary isotope effect being reasonably assumed to be small. $[\text{M}^{3+}]$ is approximately equal to the total metal ion concentration, pH, f_1 and f_3 are constants, so we have,

$k_{\text{obs}} = k_u + Kk_c$ where k_u refers to the uncatalysed reaction and K is a constant.

$$\begin{aligned} \therefore k_{\text{obs}}_{12} &= k_{u12} + Kk_{c12} \\ \text{and } k_{\text{obs}}_{13} &= k_{u13} + Kk_{c13} \end{aligned} \quad \left. \right\} \dots\dots \text{(iii)}$$

Now $k_{\text{obs}}_{12} = k_{\text{obs}}$ for the overall unenriched reaction.

$$\therefore \frac{k_{\text{obs}}_{12}}{k_{\text{obs}}_{13}} = \frac{k_{\text{obs}}}{k_{\text{obs}}_{13}} = \text{kinetic isotope effect}$$

Hence k_{obs}_{13} can be obtained. By the same argument, k_{u13} can also be determined and hence Kk_{c12} , Kk_{c13} and (hence) k_{c12}/k_{c13} , which is the kinetic isotope effect for MA^+ .

The results of these calculations are shown in Table 4.

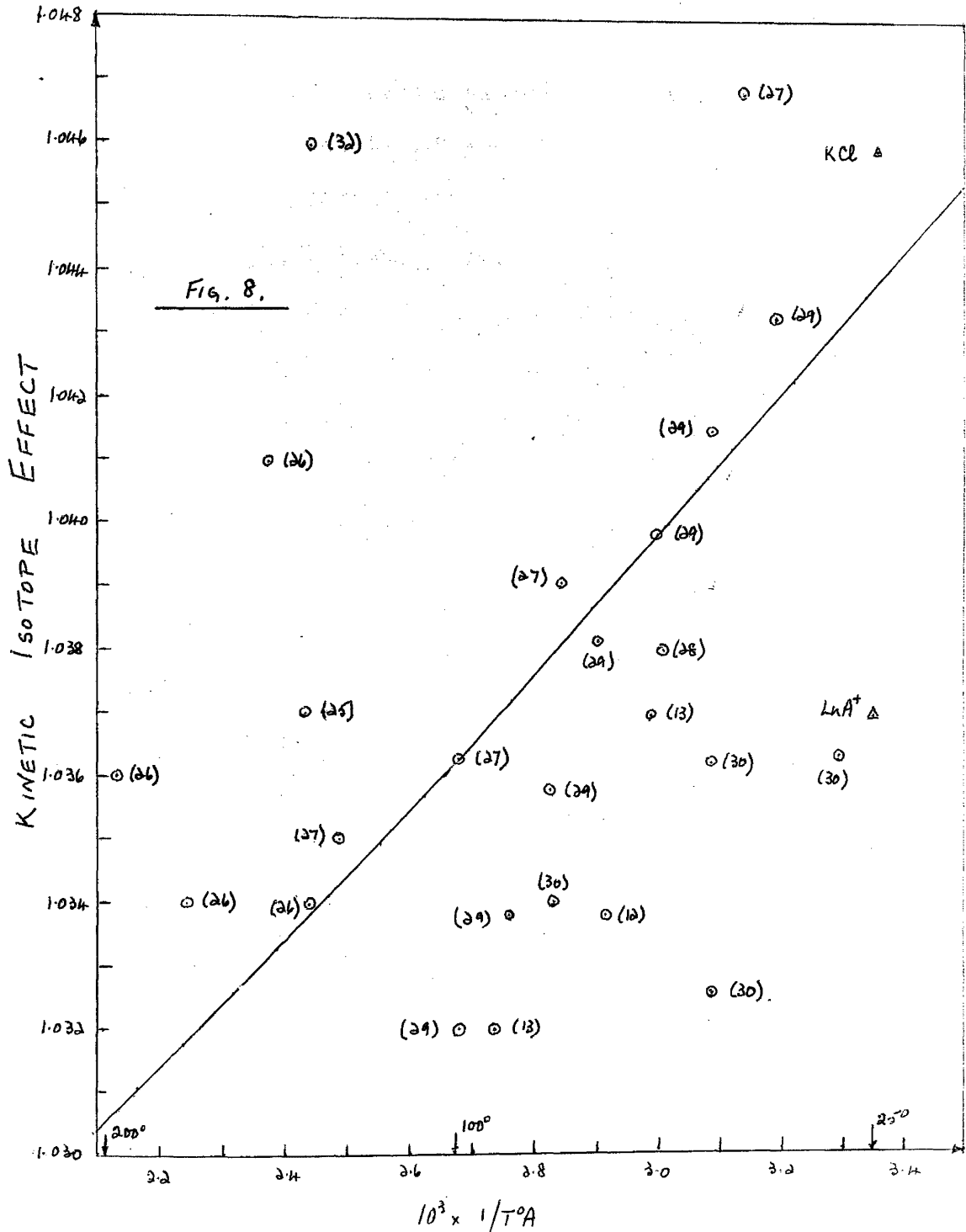
Table 4.

	$10^3 x k_{\text{obs}}_{12}$	$10^3 x k_{\text{obs}}_{13}$	$10^3 x Kk_{c12}$	$10^3 x Kk_{c13}$	k_{c12}/k_{c13}
Y	4.05	3.905	3.833	3.698	1.037
Dy	3.96	3.819	3.743	3.612	1.036
Gd	4.74	4.562	4.523	4.355	1.039
KCl	$0.217(k_{u12})^*$	$0.207(k_{u13})$	-	-	-

* new value.

The mean kinetic isotope effect for MA^+ is then 1.037 ± 0.002 from the above data. The kinetic isotope effect for the uncatalysed reaction is 1.046.

2. Comparison with theory. The theoretical value for the C¹³ kinetic isotope effect at 25° is 1.044, according to Bigeleisen (24), which comes between the uncatalysed and catalysed reactions' kinetic isotope effects. It will be shown later, in the theoretical section, that the observed kinetic isotope effect depends, inter alia, on bond force constants. Hence we may ascribe the difference between the catalysed and uncatalysed reactions' kinetic isotope effects to a difference in bond strength between the two isotopic molecules, and, in particular, to a difference between the two fissile bonds being compared. It can be shown, making various assumptions, that a fall in the force constant for the fissile bond leads to a fall in kinetic isotope effect. Hence we can put the difference in kinetic isotope effects between the uncatalysed and catalysed reactions down to a difference in force constants, caused, in turn, by the presence of M³⁺. Hence the fall in kinetic isotope effect for MA⁺ can be explained in terms of the inductive effect of the metal ion in withdrawing electrons from the labile bond and hence reducing the kinetic isotope effect by reducing the bond frequency. This hypothesis is supported by the similarity of the metal ion kinetic isotope effects, bearing in mind the nature of the catalyst ions.

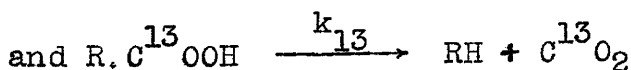
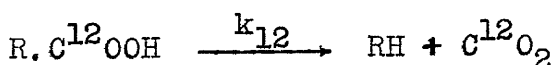


3. Comparison with C¹³ intermolecular kinetic isotope effects obtained by other workers.

A graph of kinetic isotope effect v. $\frac{1}{T_{OA}}$ is shown in Fig. 8. The results of the C¹³ work are shown as Δ -points and the curve of kinetic isotope effect v. $\frac{1}{T_{OA}}$ according to Bigeleisen (24) also drawn. The KCl reaction's kinetic isotope effect is in agreement with the general trend of experimental points; the effect of the rare earth ions is clearly observed in the lower value for their kinetic isotope effect. Not all the literature data are given in Fig. 8, various results for the decarboxylation of oxaloacetic acid in quinoline, which acts as both solvent and catalyst, being omitted. These values (33, 38) are rather higher than the usual average trend.

Conclusion.

Oxaloacetic acid has been decarboxylated at 25° in aqueous solution, alone, and also in the presence of the cations of Y, Dy and Gd, which act as catalysts via complex formation. The kinetic isotope effect for the parallel isotopically competitive reactions represented by,



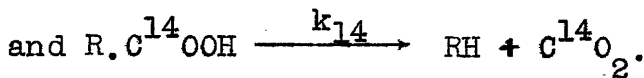
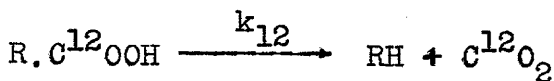
was found and evaluated in terms of the ratio (k_{12}/k_{13}) of

the two first order rate constants for the uncatalysed and catalysed reactions. The analysis was performed by measuring the isotopic content of the effluent carbon dioxide at various fixed stages in the reaction, using a mass spectrometer, and the results showed that the light (C^{12}) reaction was a few percent faster than the heavy one, in all cases. The investigation was carried out on ordinary oxaloacetic acid and also on specially prepared oxaloacetic acid, enriched to about 4% in oxaloacetic acid-1- C^{13} , similar conclusions being reached for both. The results fell into two groups, those for the uncatalysed reaction and a lower set for the catalysed reactions. The difference has been put down to an inductive effect of the metal ions, which complex with the oxaloacetic acid as shown on p. 5. The results have also been compared with theoretical and literature data.

C¹⁴ Kinetic Isotope Effects in the Decarboxylation of
Oxaloacetic Acid.

Introduction.

The object of this second part of the work was to find the kinetic isotope effect, if present, for the reaction pair,



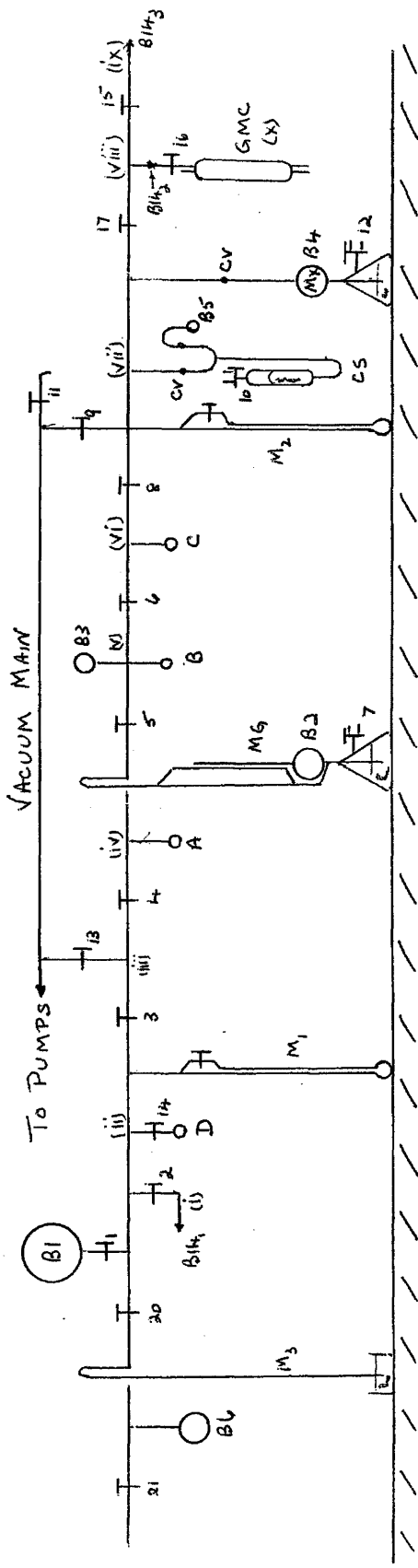
The ks are first order rate constants and the kinetic isotope effect is measured by the ratio k_{12}/k_{14} , which should be a little over unity, if a normal kinetic isotope effect is present. The reaction was performed for the acid alone, and also in the presence of the cations of Y, Dy and Gd, in turn, as before, and the kinetic isotope effects for the acid and the various complexes obtained and intercompared. In view of the C¹³ results, and indeed on the basis of the predictions given by Gelles & Reed (11), all the complexes were expected to show the same kinetic isotope effect. The C¹³ and C¹⁴ kinetic isotope effects for each species could now be studied together.

Part 1 : Preparation of C¹⁴-enriched oxaloacetic acid.

This is necessary, due to the extremely low C¹⁴ content of ordinary carbon. Due to the radioactivity of C¹⁴, precautions were taken during the preparation to prevent contamination and afterwards all the apparatus used was washed in hot caustic soda. Preliminary calculations were made of the radioactivity required, taking a figure of 4000 counts per minute (cpm) as a desirable count rate for the Geiger counter, assuming only half the radioactive effluent carbon dioxide would actually be counted, considering the probable volumes of the various parts of the vacuum line (for which see later) used in handling the radioactive carbon dioxide and taking a 5% reaction as a minimum amount of effluent carbon dioxide. The plan was to start from radioactive sodium acetate; otherwise the procedure was as previously described for the preparation of oxaloacetic acid enriched in oxaloacetic acid-1-C¹³ (see pp.22 & 23). 0.5 millicuries (0.5 mc.) of radioactivity were supplied from Amersham; the synthesis was done on about a one-quarter gm.-molar scale and checked by a preliminary pilot run. The diluent sodium acetate necessary (there was only a tiny pinch of radioactive material) was dried spread out on a clock glass in the oven at about 130° overnight: this was found to dehydrate the material easily and efficiently. The apparatus was scaled up appropriately, as compared with

the C¹³ synthesis. Brisk mechanical stirring was used during the Claisen condensation and acidification of the sodium diethyloxaloacetate enolate. Three fractions were obtained in the vacuum distillation of the diethyl oxaloacetate: the second one was small, presumably diethyl oxalate, and the third one was the diethyl oxaloacetate. The yield was about 50% here. The radioactive oxaloacetic acid produced was in about 40% overall yield, but after recrystallisation by a method due to Pedersen (23), the yield (for the first crop of crystals) was only 10%. The purity of the material was checked by titration (observed equivalent, 65.7; ideal, 66.0), gravimetric analysis (C, 36.1; H, 3.25: ideal values are C, 36.4; H, 3.05) and a manometric decomposition as before (the pressure change equalled that of Light's oxaloacetic acid) and found to be satisfactory.

Fig. 9.



M_1 , etc. are manometers, B_1 , etc. are bulbs, T , etc. are taps, MG is the McLeod Gauge, CS is the carbon disulphide store, M_x is the gas mixer, GMC is the Geiger-Müller counter, BI_4 , etc. are BI_4 joints. The sections, (i), etc. are as shown. 5mm. tubing used throughout.

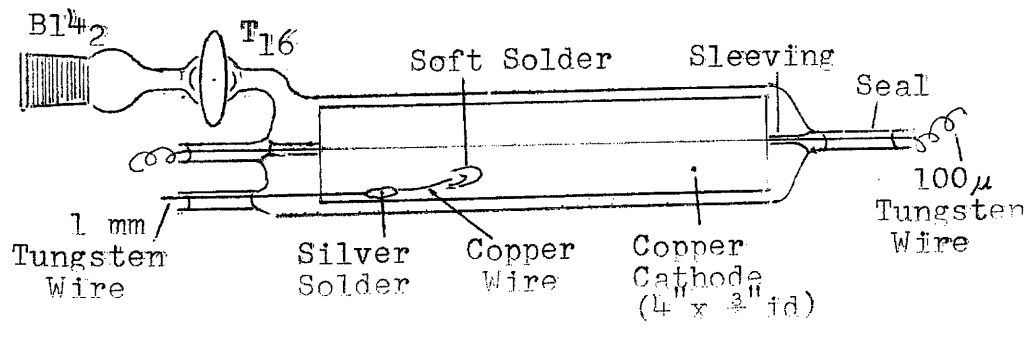
75

Part 2 : Apparatus.

The actual decarboxylations were carried out in exactly the same manner as before (see pp. 11-13), using the reaction vessel of Fig. 2. After each reaction was quenched, the vessel was connected at B_{14} , on the vacuum line shown in Fig. 9. The section containing B_6 and M_3 is for filling storage bulb B_1 with diluent carbon dioxide (from a cylinder), via a condensation and pump (to remove any volatile impurities) in B_6 , chilled in liquid air. The diluent carbon dioxide is then sublimed from B_6 chilled in acetone/Drikold, until B_1 is filled to atmospheric pressure, as noted on M_3 . The volumes of sections (ii), (iii), (v)-(viii) and (x) were found by expanding known volumes of air at known pressures into the apparatus section by section from bulbs connected at B_{14} and B_{14} . This enables calculations to be made of the correct diluent carbon dioxide and carbon disulphide pressures required for filling the counter, though this is not strictly necessary for the pressures can be found more easily empirically. The McLeod gauge measuring tube was calibrated before being assembled by filling it with mercury, weighing, and noting the length of the mercury column, measuring, using a cathetometer, from the meniscus to the outside end of the flat-ended tube. A meniscus correction was also made, assuming

the meniscus to be in the shape of a section of a sphere, so that volumes could be obtained by noting the length of the space above the mercury, when the guage is in use, from the top of the meniscus to the outside of the end of the calibrated tube. A graph of volume against length was then drawn. The carbon disulphide store was filled by vacuum distillation of some carbon disulphide from a bulb attached at $B1\frac{1}{3}$, in an obvious manner. The manometers M_1 and M_2 were fitted with taps as shown. This greatly simplified filling and enabled the closed limb to be pumped out if traces of gas got in. B_1 was a 500 ml. bulb (a larger one would have been better, since it would have required less frequent filling), B_3 and B_6 were 100 ml. each and the other small bulbs about 5-10 ml. each. B_2 and B_4 were each 250 ml. One side of each of taps T_7 , T_{10} and T_{12} was open to the air and the other connected to a common rough-vacuum main. The Geiger counter is shown in more detail in Fig. 10.

Fig. 10.



Various designs were tried and the one used in most of the work shown on the previous page (35). The volume is about 100 ml. Several counters were made as shown in Fig. 10 and tried, since not all will work satisfactorily. The cathode has to be cleaned carefully with emery paper, then Brasso and finally treated with the solutions noted in appendix D. The central wire is cleaned with emery paper before fitting. The counters were each tested by filling them with a mixture of carbon dioxide and carbon disulphide in various proportions and at various pressures until the best plateau and slope were obtained for each. The procedure in a count is described on p.37. The radioactivity for these tests was supplied by an external Co⁶⁰ source, the distance of which from the counter was varied to give the required count rate. The counter showing the best characteristics was then chosen for the C¹⁴ experiments.

The scaling equipment used in most of the work was supplied by the Radiochemistry section and consisted of a Labgear HT unit and potentiometer (type 1007) giving 2000V, with a Dynatron scalar (type 1009B) and Ericsson probe unit (type 110A). This latter was modified to give a setting of paralysis time of 1000 (i.e., 1000×10^{-6} secs.). The HT was supplemented by several HT radio batteries, giving an additional 500V and wired as shown in Fig. 11.

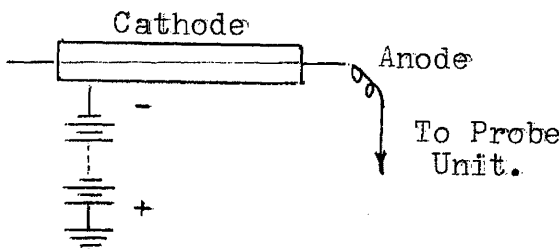


Fig. II.

Part 3 : Outline of experimental technique and theory.

As mentioned before, the reactions were carried out in the usual way, care being taken to avoid impurities by degassing each reaction solution before starting. The reactions were stopped by sudden chilling in acetone/Drikold, the reaction vessel connected at B_{14} (Fig. 9), and the whole line pumped down. A suitable quantity of radioactive carbon dioxide was then drawn into section (ii) by noting M_1 , and passed, via a condensation in bulb D and also in bulb A, to the McLeod Guage, where it was measured. A suitable pressure of diluent carbon dioxide was measured into sections (vii), (viii) and (x) from B_1 , condensed in bulb C, and the rest of the line repumped. The carbon disulphide was then expanded from the store, keeping B_5 chilled in acetone/Drikold, into sections (viii) and (x) and then condensed also into bulb C. Finally the radioactive carbon dioxide was passed from the gauge, via a condensation in bulb A, into bulb C, the mixture allowed to sublime to fill sections (vii), (viii) and (x), mixed by running the mercury up and down several times in M_2 (see Fig. 9) and the count taken. This latter was performed by connecting up the scalar and batteries, simply increasing

the voltage by 20V steps and noting the number of counts in one minute, using a stopwatch, at each step. A graph of counts per minute against volts was then drawn in each case, as shown in Fig. 12 for 25% Gd, and the standard count rate taken as, say, at 50V from the threshold of the plateau.

When calibrating the counters, the one being tested was filled with a suitable carbon dioxide/carbon disulphide mixture and the plateau found as noted above, using an γ -source (Co^{60}), the position of the source being adjusted to give about 4000 counts per minute on the plateau. The source must not be moved during a test, of course. The test was then repeated for various total pressures (obtained by running the mercury down in the gas mixer Mx - see Fig. 9).

With a sample of radioactive carbon dioxide in the counter, in order to find the activity per unit amount of radioactive effluent carbon dioxide it is necessary to consider the background radiation and the dead time of the counting apparatus. If C_0 is the observed count rate, including the background, at the chosen point on the Geiger plateau, C_T is the observed number of counts per minute, corrected for the paralysis time of the counter (i.e. the time taken by the apparatus to recover from a pulse, before it can count another pulse), C'_T is the observed count rate, corrected for both paralysis time and background and τ is the paralysis time in minutes, we have, in one minute,

Actual working time = $(1 - C_0 \cdot \gamma)$ minutes.

$$\therefore C_T = C_0 / (1 - C_0 \cdot \gamma).$$

$$\therefore C'_T = C_0 / (1 - C_0 \cdot \gamma) - B,$$

where B is the background count rate.

Now, due to the construction of the apparatus, only a fixed fraction of the radioactive carbon dioxide introduced into the counter and associated sections of the vacuum line actually registered. The total amount, however, was known, since it was measured in the McLeod Guage. Let this amount be x where x is the product of pressure and volume as measured in the gauge. Then the standard activity is defined as equal to (or proportional to) C'_T/x .

i.e., the standard activity

$$= \frac{C_0 / (1 - C_0 \cdot \gamma) - B}{x}$$

In practice the background count was very low and so need not be corrected itself for paralysis time. The x-value was corrected to 25°. Note that there is no decay correction for the C^{14} , since the rate of decay of C^{14} is so very slow that any change in the C^{14} content of the radioactive oxaloacetic acid was negligible over the time taken for this research.

Part 4 : Experimental Procedure.

To perform an experiment, the reaction chosen was carried out to the desired degree of completeness, as described already for the corresponding C¹³ work. (Note that the difference in overall rates between ordinary oxaloacetic acid and the C¹⁴-enriched material is negligible, due to the very low C¹⁴ content of even the latter). At the end the reaction vessel, with bulb kept chilled in acetone/Drikold, was connected to the vacuum line (Fig. 9) at B₁. While the reaction was in progress, the whole line, including the McLeod **gauge**, was pumped down, the mercury then run up in the gauge (by manipulating T₇) and the line filled with diluent carbon dioxide from B₁ to a pressure suitable for the counter (read M₁ or M₂). T₆ was closed and the carbon dioxide in sections (vi) - (viii) and (x) condensed in bulb C, chilled in liquid air, while the rest, in sections (ii) - (v), was pumped away. The solid carbon dioxide in bulb C was sometimes pumped to remove any traces of foreign gases which might interfere with the operation of the counter. T₈ was then closed, the carbon disulphide bulb chilled in acetone/Drikold, the store opened by running the mercury down from the check valves by manipulating T₁₀ and the carbon disulphide allowed into sections (vii), (viii) and (x) to a predetermined pressure. The small volume effect of section (vi) was ignored. The

carbon disulphide store was then closed, the carbon disulphide condensed in bulb C and T₈ reclosed. The radioactive carbon dioxide was next transferred, in an obvious manner, keeping T₃ shut, from the reaction tube and condensed in bulb D, using liquid air. The reaction vessel's stopcock and T₂ were then closed. The radioactive carbon dioxide was also usually degassed for a few moments in D. With bulb D in acetone/Drikold, the correct amount (usually 2 or 3 mm. on M₁) of radioactive carbon dioxide was then allowed to sublime into section (ii) and this passed into the McLeod gauge for measurement, via a condensation in (mercury run up in gauge) and resublimation from (from acetone/Drikold; mercury run down) bulb A. T₅ and T₁₃ were kept shut during this transfer. The mercury was then run up in the gauge, sections (iii) and (iv) pumped down and the mercury levels in the measuring and comparison limbs of the gauge adjusted by manipulating T₇ so as to make the pressure and volume lengths about equal. The successive condensation and resublimation of the radioactive carbon dioxide ensured its dryness, necessary in the operation of the counter. A convenient pressure in the gauge was usually about 5 cm. of mercury, with a volume (read from the gauge calibration graph) of about 1.5 ml. The volume was corrected to 25°C. Finally the radioactive carbon dioxide was transferred to bulb C via another condensation in bulb A. With T₆, T₁₅ and T₁₉ shut

and T_8 , T_{16} and T_{17} open, the mixture of carbon dioxide, carbon disulphide and radioactive carbon dioxide was allowed to sublime into sections (vi) - (viii) and (x) and mixed six times by running the mercury up and down in the gas mixer, M_x , by manipulating T_{12} . It may be noted that suitable values for the carbon disulphide and diluent carbon dioxide pressures were found by calibration of the counter to be about 1.5 and 13.5 cm. of mercury respectively, but these were not strict. The radioactive carbon dioxide usually registered about 1 mm. on M_2 as well. M_2 was checked, T_{16} closed, the leads to the counting equipment connected up and the mixture counted. As the voltage was increased, in steps of 20V, the edge of the plateau was usually found to be about 1800V on the potentiometer (+ 500V on the batteries) and the plateau about 100V long. At the end of the plateau the count rate increased very rapidly with increasing voltage. The number of counts per minute was noted every 20V, using a stopwatch. A typical result is given below. A background count (taken every few days) was done by filling with carbon disulphide and diluent carbon dioxide in the same way (except that no radioactive carbon dioxide was introduced) and counting.

Example : 25% Gd run.

Here the counter was filled with 13.75 cm. pressure of diluent carbon dioxide, 2.05 cm. carbon disulphide and 0.1

cm. radioactive carbon dioxide. The latter's reading on M_1 was 0.25 cm. and in the McLeod gauge it was 5.79 'cm. vol.' (i.e. 1.81 ml.) at 6.00 cm. mercury and 25° . Hence the amount of radioactive carbon dioxide was represented by,

$$P \cdot V = x = 1.81 \times 6.00 = 10.860,$$

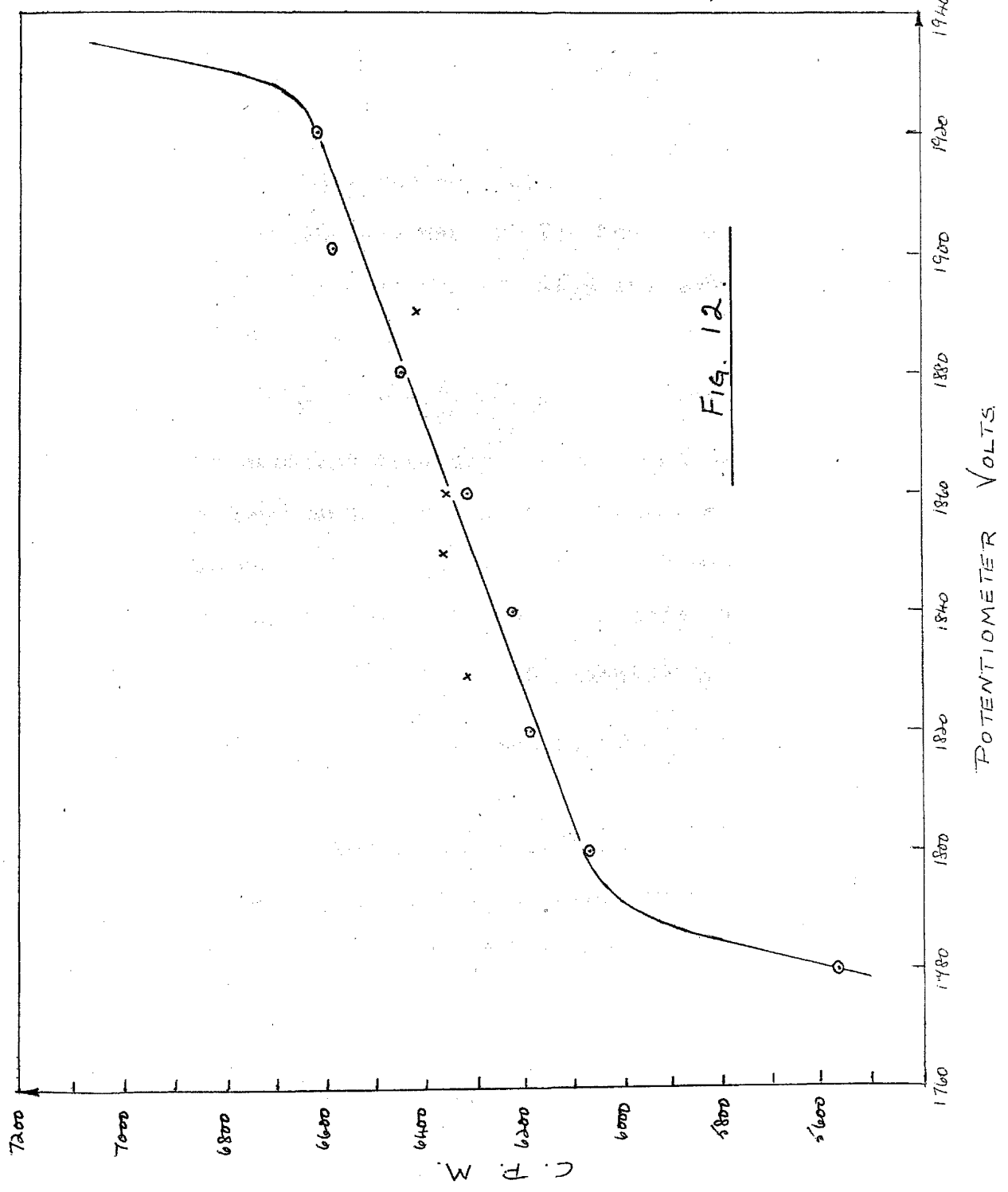
no temperature correction being necessary this time. The gases were mixed by running the mercury up and down seven times in M_x .

Counting Data :

Potentio-											
meter	volts	1760	1780	1800	1820	1840	1860	1880	1900	1920	1940
Counts per minute		227	5470	6069	6184	6220	6310	6449	6592	6615	raced

The vertical lines mark the boundaries of the plateau. In addition to the above readings, counts were taken at four other points, each for two minutes, so as to get the actual number of counts over 10,000, since when the number is large, the standard deviation is approximately given by its square root and it was desired to get the standard deviation to below 1% of the count. The four points and the results for this example are given below. The voltages are again potentiometer readings only; the absolute values are about 500V higher in each case.

Fig. 12.



Starting (i.e. threshold) voltage + 50 =	1850 V;	cpm =	6364.
Voltage at mid-point of plateau	= 1860 ;	" =	6362.
Mid-point voltage + 30 V	= 1890 ;	" =	6414.
" " " - 30 V	= 1830 ;	" =	6293.

All the data was then graphed, as shown in Fig.12. The plateau length (ΔV) was 120 V; the rise in height (ΔC) was 530 cpm. The starting cpm (C_1) was 6085 and the slope of the plateau is given by,

$$\frac{\Delta C}{C_1} \times 100 \times \frac{100}{V} = \frac{530 \times 100 \times 100}{6085 \times 120} = 7.3\%, \text{ here.}$$

The standard activity was obtained by noting, from the graph, the counts per minute at 50 V from the lower edge of the plateau. This voltage was 1850 V and the corresponding counts per minute 6300, in this case.

\therefore Time lost = $\frac{6300 \times 10^{-6} \times 10^3}{60}$ minutes in 1 minute,
since the paralysis time was set at 1000μ (i.e., 1000 millesconds),

$$\text{i.e., time lost} = 0.1050 \text{ minutes.}$$

$$\therefore C_T = 6300/(1 - 0.1050) = 6300/0.8950 = 7039.$$

The background was 190 counts per minute, so $C'_T = 7039 - 190$ = 6849 counts per minute, giving a standard activity of $6849/10.860 = 631$ at 25° .

Part 5 : C¹⁴-Results.

The kinetic isotope effect results obtained are summarised in Table 5. In taking the average for the Dy experiments the 35% value has been omitted, as being slightly high. The kinetic isotope effects were calculated using the graph of Fig.1, since the C¹⁴ content is very low (see Appendix E). A shorter table (No.6) of results is given below.

Table 6 : C¹⁴ kinetic isotope effects.

Reaction :	Y	Dy	Gd	KCl
Kinetic Isotope Effect :	1.109 ±0.007	1.107 ±0.007	1.114 ±0.008	1.132 ±0.008

The errors are standard deviations. The uncatalysed (KCl) result is a little higher than the rest, and these are all practically identical, within the limits of experimental error.

Table 5 : Results of C¹⁴ experiments.

No.	Run	N _X	N _X ^O /N _X	KIE	Mean KIE
1	10% Y	622	1.105	1.111	
2	15	622	1.105	1.114	
3	25	634	1.084	1.096	1.109±0.007
4	35	628	1.094	1.117	
5	50	640	1.073	1.105	
6	10% Dy	623	1.103	1.109	
7	15	628	1.094	1.102	
8	25	624	1.101	1.117	1.107±0.007
9	35	619	1.110	1.137	
10	50	643	1.068	1.098	
11	10% Gd	619	1.110	1.116	
12	15	620	1.108	1.117	
13	25	631	1.089	1.103	1.114±0.008
14	35	624	1.101	1.126	
15	50	639	1.075	1.108	
16	3.3%KCl	613	1.121	1.125	
17	5.0	614	1.119	1.124	
18	8.7	610	1.126	1.134	1.132±0.008
19	12.7	606	1.134	1.147	
20	19.6	616	1.115	1.129	

The N_X^O value was 687, the mean of 15 ∞ runs done during whole course of C¹⁴-experiments.

Part 6 : Discussion of C¹⁴-results.

1. The results shown in Table 6 show a definite normal isotope effect in each case, i.e., the 'heavy' reaction is slower than the 'light'. In accordance with expectation all the catalysed reactions give similar values for their kinetic isotope effects, though the result for the uncatalysed reaction is higher than the rest. If we determine the kinetic isotope effects for the metal ion complexes in the same way as before (see pp.24-27) we have, by analogy,

$$\left. \begin{aligned} k_{\text{obs}}_{12} &= k_u_{12} + K \cdot k_c_{12} \\ \text{and } k_{\text{obs}}_{14} &= k_u_{14} + K \cdot k_c_{14} \end{aligned} \right\} \dots\dots \text{(iii)}$$

Since $k_{\text{obs}}_{12} = k_{\text{obs}}$ for the overall unenriched reaction,

$$\frac{k_{\text{obs}}_{12}}{k_{\text{obs}}_{14}} = \frac{k_{\text{obs}}}{k_{\text{obs}}_{14}} = \text{kinetic isotope effect.}$$

In the same way as before we obtain the following results (Table 7):

Table 7.

	$10^3 x k_{obs_{12}}$	$10^2 \times k_{obs_{14}}$	$10^3 x K_{xx} k_{c_{12}}$	$10^3 x K_{xx} k_{c_{14}}$	$k_{c_{12}} / k_{c_{14}}$
Y	4.05	3.652	3.833	3.460	1.108
Dy	3.96	3.577	3.743	3.385	1.106
Gd	4.74	4.255	4.523	4.063	1.113
KCl	$0.217(k_{u_{12}})^*$	$0.192(k_{u_{14}})$	-	-	-

* new value.

The mean C¹⁴-kinetic isotope effect for the 1:1 complex LnA⁺ is then 1.109 ± 0.004 , taking the above data (Col. 6). The kinetic isotope effect for the KCl reaction is 1.132.

2. Comparison with theory. The theoretical value for the C¹⁴-kinetic isotope effect at 25° is 1.083, according to Bigeleisen (24) and this appears now to be low. The theory is now in better agreement with the catalysed process' kinetic isotope effect than with the uncatalysed, a complete reversal of position from that holding for the C¹³-data (see p.27). The difference in kinetic isotope effect between that for the complex LnA⁺ and that for the uncatalysed reaction is quite large: this may again be explained on the basis of the inductive effect of the complexed metal ion (see p.27), causing C-C bond weakening and a reduction

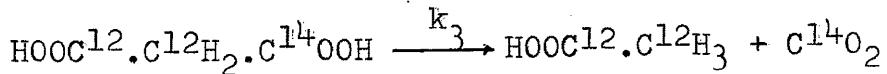
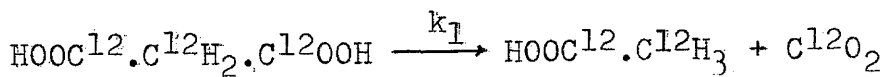
in frequency due to electron withdrawal. This will be discussed further in the theoretical section.

3. Table 8 compares the above C¹⁴ kinetic isotope effects with other values in the literature and also with the corresponding Bigeleisen (theoretical) results.

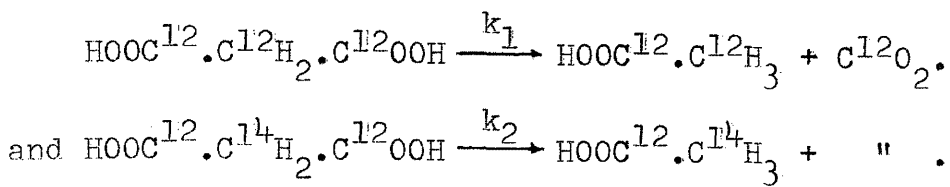
Table 8 : Experimental and Theoretical Intermolecular C¹⁴ Kinetic Isotope Effects.

Substrate	Tempera- ture	Obs. Value	Theoretical Value	Ref.
Malonic acid	154°	1.064±0.006	1.062	36.
" " (k ₁ /k ₂)	"	1.076±0.006	"	"
Mesitoic acid	60°	1.101±0.007	1.076	32.
KCl expts.	25°	1.132±0.008	1.083	-
LnA ⁺ " (mean)	"	1.109±0.004	"	-

The last two rows refer to the work presented in this thesis. Note that the decarboxylation of malonic acid is complicated by its being dibasic. The first isotope effect is for the reaction pair,



and the second for the reaction pair,



The difference between these pairs lies in the site of the heavy atom. The first order rate constants are shown according to a standard notation (25).

The balance of the experimental evidence favours a C^{14} kinetic isotope effect which is higher than the predicted value (24).

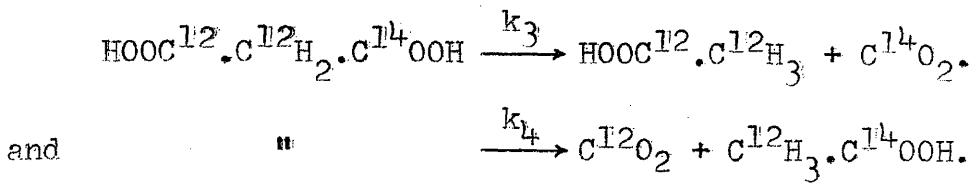
Another point often discussed in the literature is the calculation of the ratio $(\text{C}^{14} - 1)/(\text{C}^{13} - 1)$, where C^{14} stands for the C^{14} kinetic isotope effect and C^{13} for the corresponding C^{13} effect, measured under similar conditions. Table 9 shows the present state of experimental data on this subject.

Table 9 : $(\text{C}^{14} - 1)/(\text{C}^{13} - 1)$.

Substrate	Temperature	Ratio	Ref.
KCl expts.	25°C	2.9±0.4	-
LnA ⁺ "	"	2.9±0.3	-
Mesitoic Acid	60°C	2.8±0.3	28.
Malonic Acid (k_4/k_3)	140°C	2.0±0.1	37.
" " ($k_1/2k_3$:melt)	150°C	1.8±0.2	25, 26, 36.

The ratio given for the catalysed decarboxylation of oxaloacetic acid is the ratio of the mean kinetic isotope

effects for the LnA^+ complex. Note that the ' k_4/k_3 ' value for malonic acid is in the standard notation and refers to the reaction pair,



The above reaction is intramolecular; i.e. the single molecule can fission in two different ways. The $k_1/2k_3$ refers to the reaction pair noted on p. 49.

The theoretical value of the ratio is 2 and there does seem to be a trend towards this value with increasing temperature, reflecting, apparently, a corresponding decrease in the state of approximation of the theory.

Interim Conclusion on the C^{14} work.

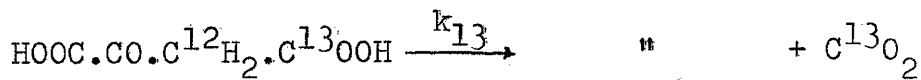
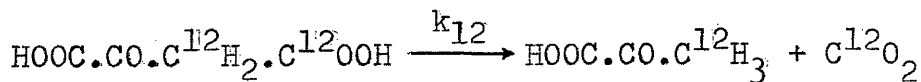
The first order decarboxylation of oxaloacetic acid enriched in oxaloacetic acid-1- C^{14} was studied to ascertain the size of the kinetic isotope effect, if present. The reaction was followed by determining the isotopic abundance of C^{14} in the effluent carbon dioxide at various fixed stages of completeness of the reaction, using a simple counting technique, convenient because of the β -radioactivity of C^{14} , and the data interpreted to yield the ratio of the two first order rate constants for the parallel isotopically competitive reactions. The acid was decarboxylated at pH = 1, alone, then in the presence of the trivalent cations of yttrium, gadolinium

and dysprosium, each in turn, and all at 25°C. These cations act as catalysts for the decarboxylation, via complex formation. From the results definite kinetic isotope effects for the uncomplexed acid and for the complexes, LnA^+ , with each of the rare earth cations, were obtained. The complexes each gave the same kinetic isotope effect, contrasting with a higher value for the uncatalysed reaction. This difference may be ascribed to the effect of the presence of the cation Ln^{3+} on the strength of the labile bond. The results have also been compared with theoretical and literature data.

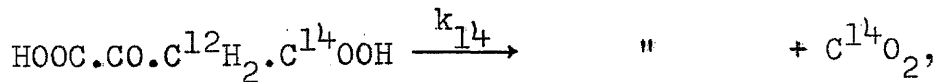
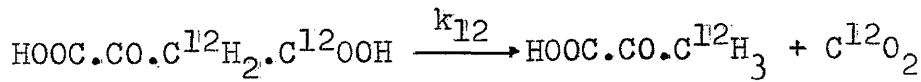
Analysis and Discussion of Carbon Isotope Effects in Decarboxylation.

Part I : Experimental Results.

1. The experimental evidence for definite normal kinetic isotope effects in the decarboxylation of oxaloacetic acid in water at 25°, alone, and then in turn in the presence of the trivalent cations of yttrium dysprosium and gadolinium, which act as catalysts via complex formation, may be summarised as shown in Table 10 below. The reaction pairs and isotopes are,



and,



where the ks are first order rate constants and the so-called C¹³ and C¹⁴ kinetic isotope effects are measured by k₁₂/k₁₃ and k₁₂/k₁₄ respectively.

Table 10.

Substrate	Active Species (pH = 1)	Magnetic Proper-ties.	C^{13} Effect	C^{14} Effect	$\frac{(C^{13}-I)}{(C^{14}-I)}$
Acid alone	Acid + mono-anion	-	1.046	1.132	2.9
" + Y^{3+}	YA^+	Dia.	1.037	1.108	"
" + Dy^{3+}	DyA^+	Para.	1.036	1.106	"
" + Gd^{3+}	GdA^+	"	1.039	1.113	"
Theoretical Value		-	1.044	1.083	1.9

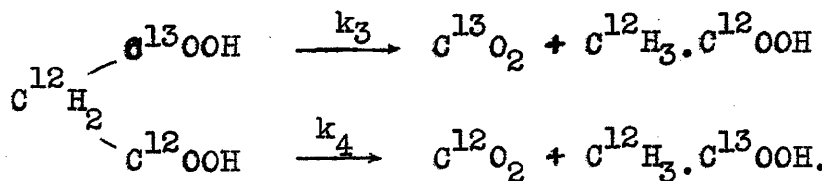
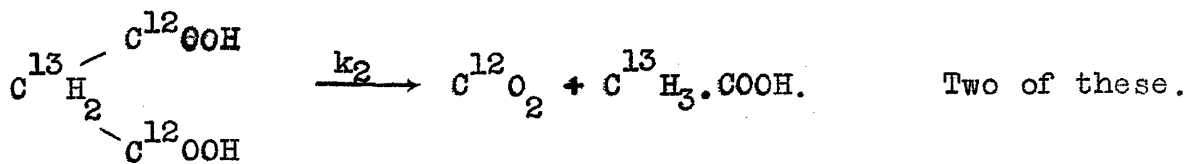
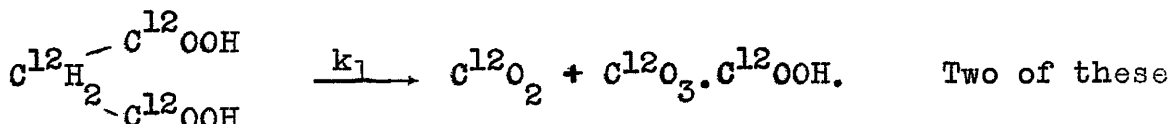
Note that the undissociated oxaloacetic acid and its monoanion are assumed to have similar kinetic isotope effects (11, 33, 38) : the carbon dioxide comes here from the undissociated acid and its monoanion in approximately equal proportions (11). A^{2-} is the dianion. 'Dia' means diamagnetic and 'para', paramagnetic.

Taking the C^{13} kinetic isotope effect first, it is clear that the LnA^+ species all show the same effect, and that this is below the value for the uncatalysed reaction. The same applies to the C^{14} effects. The C^{13} theoretical value agrees reasonably with the C^{13} effect for the uncatalysed reaction, but agreement for the C^{14} effects is poor.

The $(C^{13}-I)/(C^{14}-I)$ ratio is quite steady and is in marked disagreement with theory (24).

2. The results set out above can now be examined in conjunction with other kinetic isotope effects given in the literature.

Firstly, the C¹³ work. Early data and results were not always accurate and, e.g., one or two premature announcements were made of reverse carbon isotope effects where the heavy atom was thought to react faster than the light one but these were later strongly criticised (39,40;14,15,41,42,43). It also should be mentioned that, taking the C¹³-kinetic isotope effect for example, there are two main kinds of isotope effect. Both are exemplified by malonic acid. In a now-standard notation we have,



The existence of molecules with two or more C¹³'s in them is ignored since normally their probability would be very low in view of the low (~1.0%) C¹³ content of

ordinary carbon. The ratios k_1/k_2 and $k_1/2k_3$ measure an intermolecular kinetic isotope effect (the decarboxylation kinetic isotope effects of all monobasic acids fall into this class as well), but the ratio k_4/k_3 measures an intramolecular kinetic isotope effect. Note that in expressing these ratios, the 'lighter' (and normally faster) reaction is put in the numerator and the heavier (and generally slower) one in the denominator. This gives a ratio usually a little over unity. Similarly for the corresponding C¹⁴ notation.

(a). The present position of work on the C¹³ intermolecular kinetic isotope effect, which is the one of most interest here, is summarised in Fig. 8. As it happens, most of the results are scattered fairly uniformly on either side of Bigeleisen's theoretical curve of kinetic isotope effect plotted against $1/T^{\circ}A$ and are of the order of 3 to 5%, over the usual range of temperature in which decarboxylations are performed (12, 13, 25, 26, 27, 28, 29, 30, 31, 32). Decarboxylations of malonic acid in quinoline show effects rather higher than usual (33, 38), the quinoline acting as both solvent and catalyst. Early results for oxaloacetic acid (11) suggested isotope effects of from 6 to 10%, depending on the catalyst : the results from Table 10 are shown as -points and are clearly in disagreement with the early data. The value for the uncatalysed decarboxylation (marked KCl)

is in good agreement with the general trend (Fig.8), but the value for the catalysed reaction is much lower than might be predicted from this trend. As already discussed, this difference between the uncatalysed and catalysed reactions' kinetic isotope effects may be put down to the reductive effect of the metal ion on the electrons of the fissile bond in the complex LnA^+ . The electron withdrawal thus initiated will weaken the bond and so tend to make the system less sensitive to changes in isotopic mass. This will be discussed further in the theoretical section. The trend of the experimental kinetic isotope effects with temperature should also be noted. Fig.8 shows that at 25° the kinetic isotope effect is about 4.5%, decreasing to about 3% at 200°C .

(b) Experimental intramolecular kinetic isotope effects for malonic acid and its derivatives (measured by k_4/k_3 : see p.55) have normally been in the range 2 to 3% (25, 32, 37, 44, 45, 46), with those for malonic acid in quinoline again higher, in the range 3 to 5% (47, 48). The normal experimental values are in disagreement with Bigeleisen's predicted kinetic isotope effects, these predicted values being too high (24). In fact, according to the latest theoretical papers (24), both inter- and intra-molecular C^{13} kinetic isotope effects are equal and are shown plotted

against $1/T^{\circ}\text{A}$ in Fig. 8. Results for malonic acid in dioxane (49) show a marked temperature effect, the value being of the usual order of 2 to 3% at high temperatures, but increasing rapidly to 3 to 4% at lower ones.

(c) The second important field of carbon kinetic isotope effects here is that of the C^{14} intermolecular effect. The present experimental position is summarised in Table 8, p.49. A marked temperature effect is observable; also the theoretical values (24) are in very poor agreement with experiment.

(d) Experimental C^{14} intramolecular results have been very uneven and confusing: e.g., early work such as that of Yankwich and Calvin (50) gave values of 12% (i.e., 1.12) and 40% for the C^{14} kinetic isotope effects in the decarboxylation of malonic acid and bromomalonic acid at temperatures a little over their melting-points. The former result led Pitzer (51) to formulate a theory giving rather high isotope effects, but the value was soon challenged (52). The present position is that over the usual temperature range of $80\text{-}140^{\circ}$ in which these decarboxylations are commonly studied, the kinetic isotope effect varies from about 5.5 to 10% (37, 52, 53, 54), compared with a theoretical range of about 6 to 7.5%. Hence some results are higher than theoretical (53) and others lower (37). The data of ref. 54 show a large temperature effect, part of the work of the paper being devoted to malonic acid in quinoline.

(e) Before leaving this review of experimental data, it is desirable to mention temperature effects and the relationship between C¹³ and C¹⁴ kinetic isotope effects. Most workers have obtained temperature effects higher than those predicted by Bigeleisen (13, 27, 29, 30, 33, 38, 47, 48, 49, 53, 54), agreement being observed in only a few cases (26, 30, 32), though some of this latter work has been criticised as being unreliable (27).

(f) The relationship between C¹³ and C¹⁴ kinetic isotope effects has already been given (pp. 50 & 54) and some experimental results listed (Tables 9 & 10). The theoretical value (24) is 1.9, but it has been found (28, 44, 46) that the ratio is decidedly greater than this: this conclusion is also supported by the results in this thesis. However there is some contradictory evidence (25, 26, 36) in favour of a value of about 1.9. Note that the ratio (C¹⁴-I)/(C¹³-I) is calculated for values of C¹³ and C¹⁴ obtained for the same substrate under identical in each case and for the same effect (i.e., inter- or intramolecular).

Part 2 : General Theoretical Section.

a) The general idea here is that using the basic transition state theory as enunciated by Glasstone, Laidler & Eyring (55), it is possible to work out the ratio of two "isotopic" rate constants. If k_r is the rate constant, k the Boltzmann constant, x the transmission coefficient, T the absolute temperature, h Planck's constant and K^1 the equilibrium constant between the activated state molecules and the reactants, we have,

$$k_r = \frac{kT x K^1}{h} \quad \dots \dots \dots \quad (i)$$

$$K^1 \text{ is given by, } K^1 = Q^*/Q_A \cdot Q_B \cdot Q_C \quad \dots \dots \quad (ii)$$

where Q^* is the partition function for the activated complex, omitting the degree of freedom along the reaction coordinate and the other Q s refer to the reacting species. If we take two isotopic species, denoted by subscripts 1 and 2, with rate constants k_1 and k_2 , we find

$$\frac{k_1}{k_2} = \frac{x_1}{x_2} \cdot \frac{Q_1^* \cdot Q_{A_2} \cdot Q_{B_2} \cdot Q_{C_2}}{Q_2^* \cdot Q_{A_1} \cdot Q_{B_1} \cdot Q_{C_1}} \quad \dots \dots \dots \quad (iii)$$

Hence, if we can calculate Q_1/Q_2 , we can find k_1/k_2 . It can be shown (55, 57) that the ratio of two partition functions can be written in the form,

$$\frac{Q_2}{Q_1} = \frac{s_1}{s_2} \left(\frac{I_{A2}}{I_{A1}} \frac{I_{B2}}{I_{B1}} \frac{I_{C2}}{I_{C1}} \right)^{1/2} \cdot \left(\frac{M_2}{M_1} \right)^{3/2} \cdot \prod_{i=1}^{3n-6} e^{\frac{(v_{1i} - v_{2i})hc/2kT}{kT}} \cdot \frac{(1-e^{-\frac{hc\nu_{1i}}{kT}})}{(1-e^{-\frac{hc\nu_{2i}}{kT}})}$$

.....(iv)

where the ss are the symmetry numbers of the molecules, the Is the moments of inertia about the three principal axes of the n-atomic molecule, the Ms molecular weights and the s the fundamental vibrational frequencies in cm^{-1} , assuming these vibrations to be harmonic.

It was shown by Teller and Redlich (58) that,

$$\left(\frac{I_{A2}}{I_{A1}} \frac{I_{B2}}{I_{B1}} \frac{I_{C2}}{I_{C1}} \right)^{1/2} \cdot \left(\frac{M_2}{M_1} \right)^{3/2} \cdot \prod_j^n \left(\frac{m_{1j}}{m_{2j}} \right) \cdot \prod_i^{3n-6} \left(\frac{\nu_{1i}}{\nu_{2i}} \right) = 1 \quad \dots \dots \dots \text{(v)}$$

(See Appendix F for a demonstration proof of the above relationship for a simple diatomic molecule). In the above, the ms are the masses of the j atoms.

Hence, multiplying both sides of (iv) by $\prod_j^n (m_{1j}/m_{2j})$ and allowing for the (ν_{1i}/ν_{2i}) product term in the left hand side, we have,

$$\begin{aligned} \prod_j^n \left(\frac{m_{1j}}{m_{2j}} \right)^{3/2} \cdot \frac{Q_2}{Q_1} &= \frac{s_1}{s_2} \cdot \prod_i^{3n-6} \left(\frac{\nu_{2i}}{\nu_{1i}} \right) e^{-(u_{1i} - u_{2i})/2} \cdot \frac{(1-e^{-u_{1i}})}{(1-e^{-u_{2i}})} \\ &= f, \text{ say.} \quad \dots \dots \dots \text{(vi),} \end{aligned}$$

where $u = hc\nu/kT$.

For linear molecules, $(3n-6)$ is replaced by $(3n-5)$. If the subscript 1 refers to the lighter molecule, and

$u_1 = u_2 + \Delta u$, and u_i refers to the heavier molecule (i.e. u_{2i} is replaced, for simplicity by u_i)

$$f = \frac{s_1}{s_2} \cdot \prod_i^{3n-6} \frac{u_i}{u_i + u_f} \cdot e^{\frac{\Delta u_i/2}{(1 - e^{-u_i})}} \cdot \frac{(1 - e^{-(u_i + \Delta u_i)})}{(1 - e^{-u_i})} \quad \dots \text{(vii)}$$

For $\Delta u \ll 1$, which holds at normal temperatures for all elements except hydrogen,

$$\begin{aligned} f &= \frac{s_1}{s_2} \prod_i^{3n-6} (1 + G(u_i) \Delta u_i) \\ &= 1 + \sum_i^{3n-6} G(u_i) \Delta u_i \quad \dots \text{(viii),} \end{aligned}$$

where $G(u) = 1/2 - 1/u + 1/(e^u - 1)$ and has been tabulated for varying values of u (57). See Appendix G for proof of this step.

Q_2^*/Q_1^* can be evaluated similarly, allowing for the degree of freedom missing in the vibrational partition function; in a similar notation to the above,

$$\prod_j^n \left(\frac{m_{1j}}{m_{2j}} \right)^{3/2} \cdot \frac{Q_2^*}{Q_1^*} = \frac{s_1^*}{s_2^*} \cdot \prod_i^{3n-6} \left(\frac{u_{2i}^*}{u_{1i}^*} \right) \cdot \prod_i^{3n-7} \left(e^{\frac{\Delta u_i^*/2}{(1 - e^{-u_{1i}^*})}} \cdot \frac{(1 - e^{-u_{1i}^*})}{(1 - e^{-u_{2i}^*})} \right) \dots \text{(ix)}$$

A pair of vibrations in the first product on the right hand side are along the decomposition coordinate. Factorising them out and designating them by u_{1L}^* and u_{2L}^* , we find the right hand side of equation (ix) becomes,

$$\frac{s_1^*}{s_2^*} \cdot \left(\frac{u_{2L}^*}{u_{1L}^*} \right) \cdot \prod_i^{3n-7} \left(\frac{u_{2i}^*}{u_{1i}^*} \right) \cdot e^{\Delta u_i^*/2} \cdot \frac{(1 - e^{-u_{1i}^*})}{(1 - e^{-u_{2i}^*})} = \left(\frac{v_{2L}^*}{v_{1L}^*} \right) \cdot f^*, \text{ say,}$$

where the factorised pair are now in the cm^{-1} notation.

Hence, returning to equation (iii), we find,

$$\frac{k_1}{k_2} = \left(\frac{v_{1L}^*}{v_{2L}^*} \right) \cdot \frac{f_A \cdot f_B \cdots x_1}{f^* \cdot x_2} \quad \dots \dots \dots \quad (x),$$

cancelling all the masses m , by stoichiometry.

For only one isotopic substituent and small Δu we can write,

$$\begin{aligned} \frac{k_1}{k_2} &= \left(\frac{v_{1L}^*}{v_{2L}^*} \right) \cdot \frac{f_A \cdot x_1}{f^* \cdot x_2} \\ &= \frac{s_1 s_2^* x_1}{s_2 s_1^* x_2} \cdot \left(\frac{v_{1L}^*}{v_{2L}^*} \right) \cdot \left(1 + \sum_i^{3n-6} G(u_{1i}^*) \Delta u_i - \sum_i^{3n-7} G(u_{2i}^*) \Delta u_i^* \right) \dots (xi) \end{aligned}$$

For carbon isotope effects, the variation in vibrational frequencies is small, so the s_1/s_2 terms are assumed to cancel, to a good approximation. The x_1/x_2 term is also assumed to cancel. Although the above equation is derived for gas reactions, the effect of vapour pressure correction terms is neglected, being very small (24). The resulting equation, obtained originally by Bigeleisen (56) is the one most familiar in carbon kinetic isotope work.

(b) The first factor $(\nu_{1L}^{\neq}/\nu_{2L}^{\neq})$, in the Bigeleisen equation, is known as the frequency factor, or temperature independent factor (TIF) and the second as the temperature dependent factor (TDF).

i.e., $k_1/k_2 = \text{kinetic isotope effect} = (\text{TIF}) \times (\text{TDF}) \dots \text{(xii)}$

The calculation of the temperature independent factor has presented some difficulties. Strictly, it can only be evaluated from a knowledge of the potential energy surface for the reaction (55, 59). However, Slater (60) found that if the reaction only involves fission of a single bond between two atoms A and B, then,

$$k_1/k_2 = (\mu_2/\mu_1)^{\frac{1}{2}} \dots \text{(xiii)}$$

where $\mu = m_A \cdot m_B / (m_A + m_B)$.

For a molecule, in which the bond between A and B is broken, if we take the transition state as involving movement of atoms A and B only, and no movement of other atoms, then it is the practice (61) to put,

$$(\nu_{1L}^{\neq}/\nu_{2L}^{\neq}) = (\mu_2/\mu_1)^{\frac{1}{2}} \dots \text{(xiv)}$$

Some justification for this can be derived by noting that at high temperatures the Bigeleisen equation becomes,

$$k_1/k_2 = (\nu_{1L}^{\neq}/\nu_{2L}^{\neq}).$$

A modification which has been used (24) is to put A and B equal to the massive molecular fragments between which the bond to be broken is situated.

Before leaving this topic, the decarboxylations of malonic acid in quinoline, which acts as both solvent and catalyst, may be mentioned (33, 38, 47, 48, 54). All the kinetic isotope effects found for the decarboxylation of the undissociated acid and monoanion (the latter produced by having the acid in the presence of base) have been higher than those observed for the acid in the absence of quinoline or for other decarboxylations. The differences have been interpreted in terms of solvent effects (24, 29, 49, & as above), particularly with respect to effects on the temperature independent factor. It is possible to put the variation of kinetic isotope effect with absolute temperature in the form,

$$\log \left(k_1/k_2 \right)_{\text{obs}} = a/T + b = \log (\text{TIF}) + \log (\text{TDF}),$$

where a and b are constants from the simple Arrhenius rate equation and using equation (xii) on p. 64. Various complicated polycentric models have been proposed to give suitable temperature independent factors which can be compared with that obtained from the term b in the above equation for catalysed and uncatalysed reactions.

An example of the calculation of the temperature independent factor for ethane is given in Appendix H. Note that in most (but not all) "isotopic" reactions, the "light" atom or molecule will react more quickly than the heavy one,

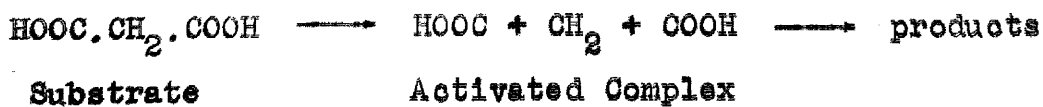
this being reflected in both the temperature independent factor and temperature dependent factor being slightly greater than unity.

Part 3 : Application of kinetic isotope effect theory to decarboxylations.

To do this, it is necessary to make some intelligent guesses about the various changes occurring due to isotopic substitution in both substrate and activated complex. There are two main schools of thought, the first led by Bigeleisen and the second by Pitzer, of which the former has been the more successful.

The Bigeleisen Approach.

1. Much of the early work on kinetic isotope effects was done on the thermal decarboxylation of malonic acid. The various possible bond fissions are shown on p.55, for the C¹³ case. One of the early models for the reaction was,



Note how both C-C bonds were assumed to be loosened in the transition state.

a) Intramolecular kinetic isotope effects. Here the G(u), Δu term in equation (xi) was zero, since only

one molecule was considered. The $G(u^*)\Delta u^*$ term was also zero, since Bigeleisen considered skeletal vibrations to be reduced to zero in the activated complex and the remaining vibrations of the species to be unaffected. Hence the intramolecular kinetic isotope effect reduced to,

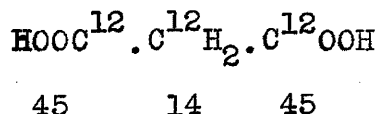
$k_4/k_3 = (\mu_3/\mu_4)^{\frac{1}{2}}$ in the standard notation (p.55), and following Slater.

$$\text{Here } \frac{1}{\mu_3} = \frac{1}{12} + \frac{1}{13} \text{ and } \frac{1}{\mu_4} = \frac{1}{12} + \frac{1}{12}$$

$$\text{Hence } k_4/k_3 = 1.020, \text{ and was temperature independent.}$$

b) Intermolecular kinetic isotope effects ($k_1/2k_3$).

Difficulties now arose, since the u and u^* terms had to be evaluated and the Δu s found. The $G(u^*)\Delta u^*$ term was eliminated as before, leaving only the substrate, whose structure was approximated by



with molecular fragment masses as shown. In the calculations two further approximations were made: firstly, the observed skeletal frequencies were used, instead of the fundamentals, and secondly, the frequency shift was calculated for the mass shift, 45-14-45 \longrightarrow 45-14-46. The resulting $\sum G(u)\Delta u$ term was then divided by two to obtain the temperature dependent part of the kinetic isotope effect

for the actual shift, 45-14-45 → 45-14-46.

The frequency shift calculations are given in Appendix I. The results are,

	c^{12}	c^{13}
w_1	756 cm^{-1}	754 cm^{-1}
w_2	230 "	228 "
w_3	905 "	903 "

The ws refer to the use of observed frequencies instead of fundamentals. Equation (xi) can now be applied, following Bigeleisen. The us were calculated for a temperature of 137.5° , using the formula,

$$u = hcw/kT = 1.438w/T = 3.503 \times 10^{-3}w,$$

where $0^\circ\text{C} = 273.2^\circ\text{A}$, $h = 6.624 \times 10^{-27}$, $c = 2.998 \times 10^{10}$ cm/sec (the velocity of light) and $k = 1.380 \times 10^{-16}$ ergs/degree (Planck's constant) (see Herzberg, ref. 62, p. 538).

∴ we have,

Table II.

w_{12} (cm^{-1})	u_{12}	w_{13} (cm^{-1})	u_{13}	$G(u_{13})$	Δu	$G(u_{13})\Delta u$
756	2.648	754	2.641	0.198	0.007	0.0013
230	0.806	228	0.798	0.066	0.008	0.0005
905	3.170	903	3.163	0.232	0.007	0.0015
						0.0034

The $G(u)$ terms can either be evaluated from the original equation (see p. 62) or obtained from Bigeleisen &

Mayer's tables (57).

The temperature independent factor was again 1.020 and, following Bigeleisen, the temperature dependent factor is $(1 + 0.0034/2) = 1.0017$.

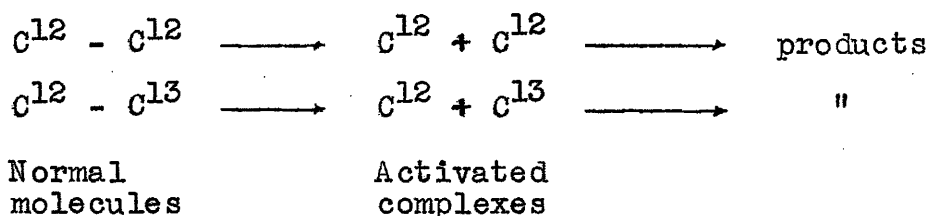
∴ the intermolecular C¹³ kinetic isotope effect for malonic acid at 137.5°C is $1.0017 \times 1.020 = 1.022$.

This theory accounted for the intramolecular kinetic isotope effect fairly well, but gave low results when used to predict intermolecular kinetic isotope effects. In fact, Bigeleisen admitted (61) that the model had only one virtue, namely, that calculations could readily be made, and in the same paper he gave a new and more successful model, with a review of C¹³ inter- and intramolecular kinetic isotope effects up to 1952.

2. This new model not only gave better results, but also simplified the calculations and removed the anomaly (see above) of considering atomic particles for the temperature independent factor (following Slater) and massive fragments for the temperature dependent factor.

(a) Taking the C¹³ effect again, for example, we find the intramolecular C¹³ effect is unchanged at 1.020 and again temperature independent. In fact, according to the intramolecular treatment, the intramolecular kinetic effect is model-independent as well.

(b) For the intermolecular effect, all the frequencies in the activated complex are assumed to be the same as those in the normal molecule, except for the C-C stretching frequency, which becomes a translation. Hence these frequencies cancel, since they will appear in both the $\sum G(u) \cdot \Delta u$ and $\sum G(u') \cdot \Delta u'$ terms. The reaction pair is then virtually,



A value of 900 cm^{-1} was used for the $\text{C}^{12}-\text{C}^{12}$ stretching frequency. Let us recalculate the C^{13} inter-molecular kinetic isotope effect at 137.5°C . Items in the calculation are shown in Table 12.

Table 12.

w_{12}	u_{12}	w_{13}	u_{13}	$G(u_{13})$	Δu	$G(u_{13})\Delta u$
900 cm^{-1}	3.152	882.5	3.091	0.224	0.061	0.0137

The frequency shift from ω_{12} to ω_{13} is for the change from a $C^{12}-C^{12}$ bond to a $C^{12}-C^{13}$ bond and is calculated using the theory for a simple diatomic molecule we have,

$$\frac{w_{13}}{w_{12}} = \left(\frac{u_{12}}{u_{13}}\right)^{\frac{1}{2}} = 1/1.0198$$

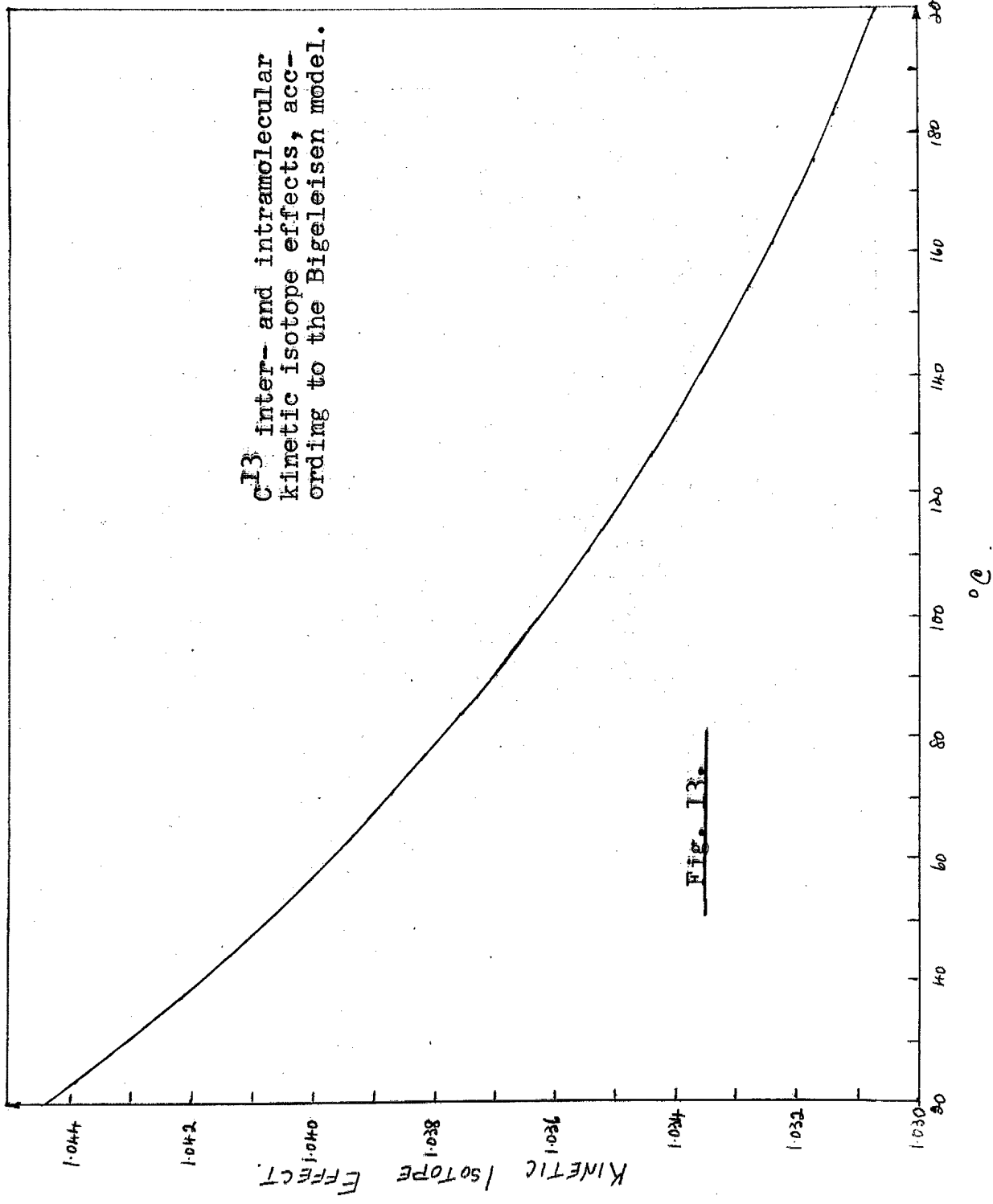
$$\text{and hence } w_{13} = 900/1.0198 = 882.5 \text{ cm}^{-1}.$$

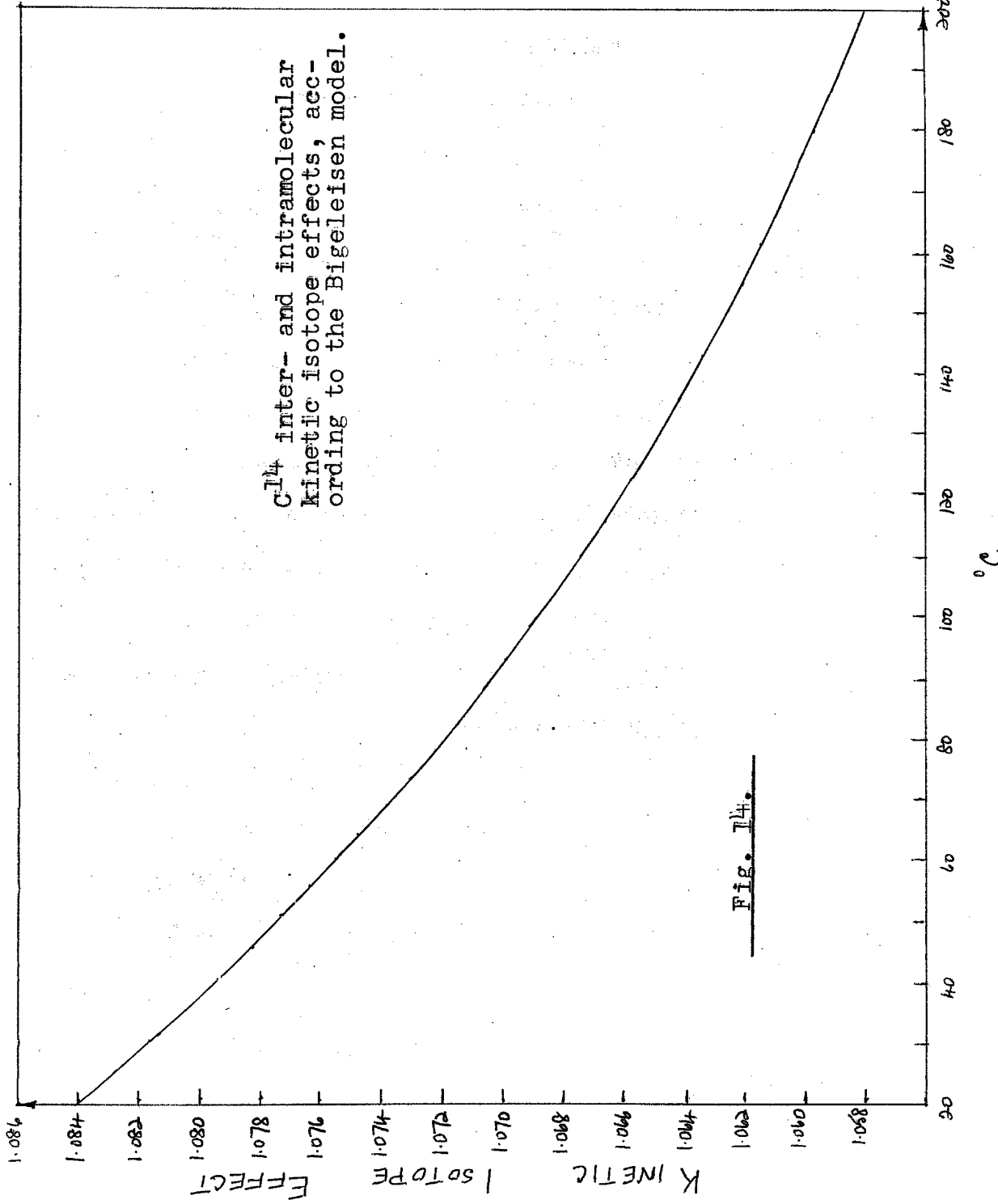
The u terms are found as before and similarly for the $G(u)$ term.

The intermolecular C^{13} isotope effect is then given by,

$$1.0198/\bar{I} + 0.0137 - \underline{07} = 1.0338.$$

Compare this value of $k_1/2k_3$ with the value of 1.022 obtained previously for the same circumstances. Note that using this new model Bigeleisen predicted that $k_1/2k_3$, i.e., the C^{13} intermolecular kinetic isotope effect, would be the same for all C-C fissions, depending only on the temperature (and on the C-C frequency chosen) and that the intramolecular effect would be independent of bond frequency, temperature and model. This latter prediction was completely revised later to conform with a suggestion by Pitzer (51) which was criticised at the time the new model was brought forward (61). The point is, that for the intermolecular kinetic isotope effect, Bigeleisen (61) considered only C-C fission, but for the intramolecular effect he still relied on the old model for the complete malonic acid molecule. In fact, if the intramolecular kinetic isotope effect is considered on the basis of C-C fission only, like the intermolecular effect, $k_4/k_3 = k_1/2k_3$ and k_4/k_3 is temperature dependent. The first hint of this third plan for malonic acid comes in a paper (64) wherein Bigeleisen and Wolfsberg show that malonic acid -2- C^{14} ($HOOC^{12}C^{14}H_2C^{12}OOH$) should decarboxylate exactly twice as fast as $C^{14}O_2$ is evolved from malonic acid

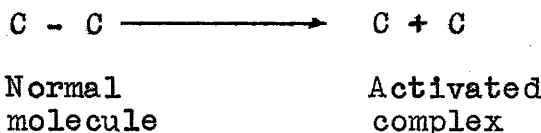




-1-C^{14} (cf. the results of Ropp & Raaen, 36).

3. The revised improved model for malonic acid (24).

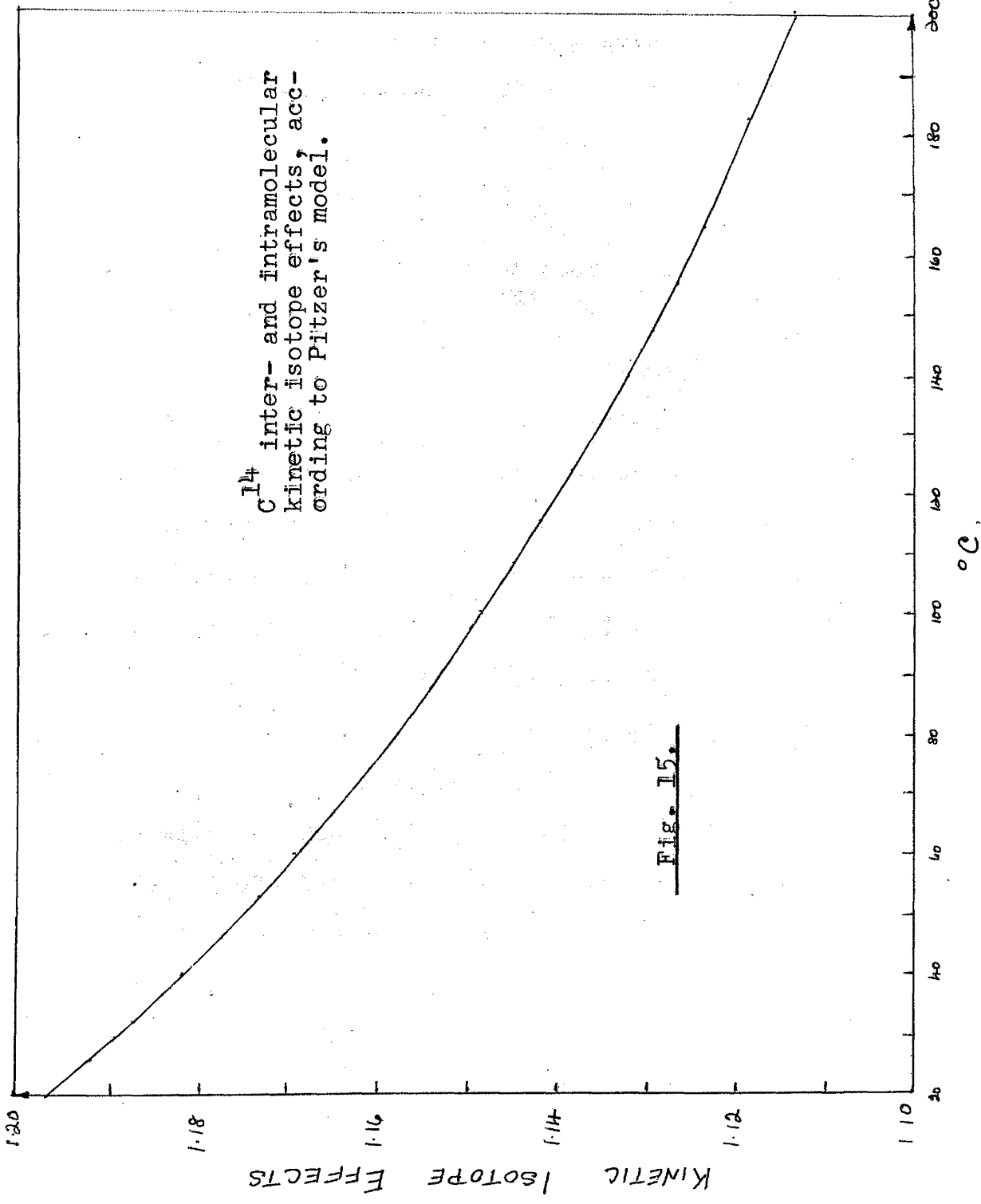
The model is the same, i.e., virtually,



The temperature independent factor is the same, namely, 1.01980. The isotopic shift in the C-C stretching frequency (taken as 900 cm^{-1}) is again given by the reduced mass relationship. In the temperature dependent factor, the $G(u^\ddagger) \Delta u^\ddagger$ term is again zero, leaving only the $G(u) \Delta u$ term to be evaluated. The intermolecular C^{13} kinetic isotope effect for 137.5°C , e.g., remains the same at 1.034, but now the intramolecular kinetic isotope effect has the same value. Furthermore, $k_1/2k_4$ and $k_2/2k_3$ are both unity (see p.55). In fact, to sum up,

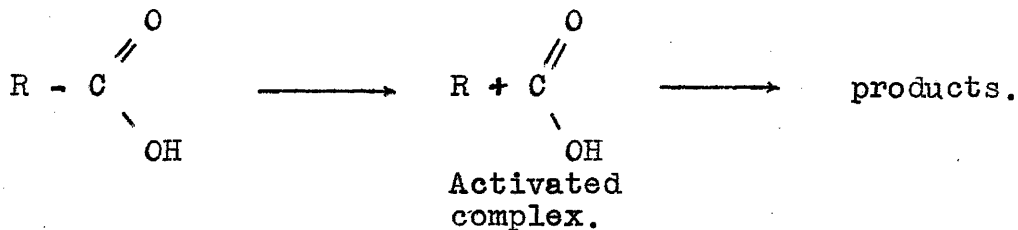
$$\begin{aligned} k_1/k_2 &= k_1/2k_3 = k_4/k_3 = 1.034 \\ \text{and } k_1/2k_4 &= k_2/2k_3 = 1. \end{aligned}$$

This theory was been used as a basis for comparison with experimental results in this thesis. Graphs of the C^{13} and C^{14} kinetic isotope effects against temperature are shown in Figs.13 & 14 respectively.



Pitzer's Model (51).

The main paper is noted in reference 51 and deals with the C¹⁴ kinetic isotope effect. The model is,



R, O and OH were all given effective masses of 16. C is 12 or 14. In the activated complex the C=O and C-OH bonds were given normal frequency values, according to Pitzer (though the force constants for these bonds need not be known). The bending constant for the CO.OH complex was put equal to zero. The appropriate formulae for working out the isotopic frequency shifts are given by Herzberg (62) and Kohlrausch (65). Pitzer (51) gives a list of C¹² and C¹⁴ frequencies and these were used to obtain C¹⁴ kinetic isotope effects (see Fig. 15) in the usual way. A demonstration calculation is given in Appendix J. The corresponding C¹³ kinetic isotope effect was obtained roughly by noting the value of

$$(C^{14} - 1)/(C^{13} - 1)$$

from the corresponding Bigeleisen calculations (over the range 20°C to 200°C the ratio ran from 1.895 to 1.897) and using this value to obtain the Pitzer C¹³ kinetic isotope

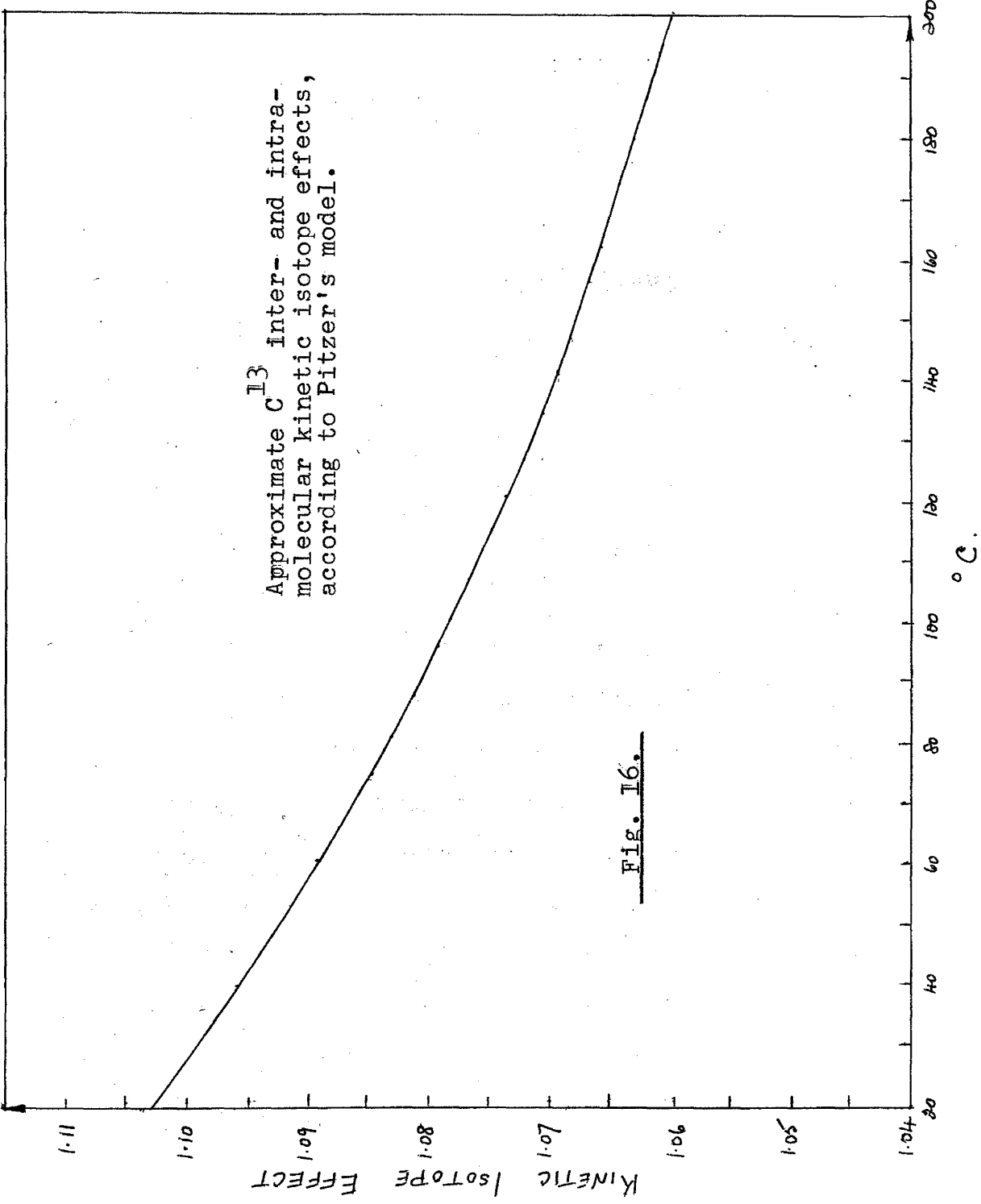


Fig. 16.

effect for each temperature: the results are given in Fig.16. It should be noted that this theory gives a predicted value for both inter- and intramolecular kinetic isotope effects, the two values being equal as in Bigel-eisen's revised model (24).

Part 4 : The Paramagnetic Catalysis Theory.

Working from relatively limited data, Fitzer & Gelles in 1953 (4) suggested that a possible cause for the deviation of the ratio

$$(C^{14} - 1)/(C^{13} - 1)$$

from about 2 lay in the paramagnetic properties of C^{13} , which has a nuclear spin. If we assume, they said, that this paramagnetism gives rise to a catalytic effect, then in the ratio k_{12}/k_{13} , k_{13} will be "too large", the ratio "too small" and hence the above expression greater than 2. They checked this hypothesis by carrying out various decarboxylations in the presence of paramagnetic ions and were able to show that these ions in fact exhibited a "super-catalytic" effect, i.e., a catalytic effect greater than that inferable from a comparison between these ions and other non-paramagnetic ions of similar size, charge and association constants (4, 5, 6). Preliminary work on the C^{13} kinetic isotope effect in the decarboxylation of oxalo-acetic acid (11) showed that the diamagnetic-ion catalysed

reaction had a "usual" kinetic isotope effect, i.e., one equal to the kinetic isotope effect for the uncatalysed reaction and of the order of 5%, but the paramagnetic-ion catalysed decarboxylation had a kinetic isotope effect of about 10%. This was put down to a paramagnetic "super-catalysis" of both the C¹²-C¹² and C¹²-C¹³ bonds whereby both numerator and denominator of k_{12}/k_{13} were increased, thus tending to raise the ratio, already greater than unity, and so to give a value of 2 for the expression on the previous page; i.e., all the usual C¹³ kinetic isotope effects were regarded now as "abnormal" due to the C¹³ paramagnetic effect and only when this effect was neutralised, as in the experiments described, could the "true" C¹³ kinetic isotope effect be observed.

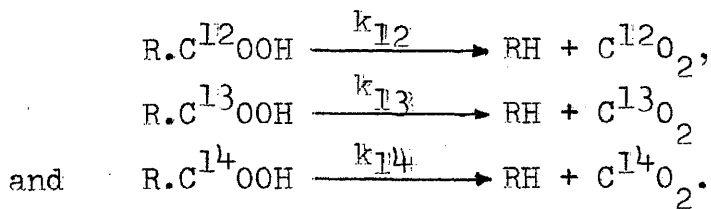
In an analogous way, C¹⁴ kinetic isotope effects were expected to remain unaffected by any catalysts, paramagnetic or otherwise, since C¹⁴ has no nuclear spin.

It should be noted that one of the weaknesses of this theory is that the C¹³ paramagnetism and the paramagnetism of Dy³⁺, e.g., arise from two entirely different causes; in the first case the effect is due to nuclear spin, as already noted, and in the second to unpaired 4f electrons, which create a magnetic moment due to their spin and orbital motion. Thus the latter phenomenon would be expected to show

a more intimate association with reactions than the former, on a purely chemical basis (66; Ch. 5).

Part 5 : Final Summary and Conclusions.

Kinetic isotope effects in the decarboxylation of oxaloacetic acid were studied at 25° in aqueous solution for the acid alone, and then in the presence of the cations of yttrium, dysprosium and gadolinium, which act as catalysts via complex formation. Both acid and complexes decompose by known mechanisms with first order kinetics and at convenient rates. The three isotopes investigated were C¹², C¹³ and C¹⁴, and the reactions were,



The purpose of the work was to show the presence of an isotope effect for both the C¹³ and C¹⁴ reactions, to investigate the effect of the catalytic metal ions and obtain values of the isotope effect for the various decarboxylating species, to ascertain if there was any possible effect due to the paramagnetic ions of dysprosium and gadolinium, in view of the known paramagnetism of C¹³, caused by its nuclear spin, and to compare experimental results with theoretically calculated kinetic isotope effects.

Ordinary carbon contains about 1% of C¹³, so ordinary oxaloacetic acid was used to determine the first kinetic isotope effect, i.e., the ratio k_{12}/k_{13} . This was done by analysing the purified effluent carbon dioxide from the reaction by means of a mass spectrometer. The reaction involving the heavy isotope lags behind the light one, so the carbon dioxide appears to have an abnormally low C¹³ content and from this k_{12}/k_{13} can be calculated.

The experiments were repeated using oxaloacetic acid enriched in oxaloacetic acid-1-C¹³ to about 4%, in order to facilitate the mass-spectrometric measurements. This enriched material was prepared from enriched barium carbonate via a Grignard reaction, giving enriched sodium acetate. The acetate was converted into ethyl acetate and thence diethyloxaloacetate obtained by means of a Claisen condensation with diethyl oxalate. The enriched oxaloacetic acid was obtained in a satisfactory state of purity by acid hydrolysis of the diethyl ester. Isotope effects similar to those already observed for ordinary oxaloacetic acid were found on repeating the experiments with the enriched material.

The k_{12}/k_{14} ratios were obtained using oxaloacetic acid enriched in oxaloacetic acid-1-C¹⁴. The preparation was the same as before for oxaloacetic acid enriched in oxaloacetic acid-1-C¹³, but started from labelled sodium

acetate. Since C¹⁴ is β-radioactive, samples of effluent carbon dioxide were analysed by counting measured volumes in a Geiger counter, using a standard technique, k_{12}/k_{14} being derived in a manner similar to that used for k_{12}/k_{13} .

The results of the work showed the presence of definite isotope effects and these are summarised below:

Reaction	Uncatalysed	YA ⁺	DyA ⁺ (p)	GdA ⁺ (p)
k_{12}/k_{13}	1.046	1.037	1.036	1.039
k_{12}/k_{14}	1.132	1.108	1.106	1.113.

Under the reaction conditions the most important species in the catalysed reactions are the complexes shown between the trivalent cations and the dianion A²⁻ of oxalo-acetic acid. (p) indicates the paramagnetic ions.

It is clear that the rates of the three isotopically labelled species are in the order $k_{12} > k_{13} > k_{14}$ in all cases. The C¹³ kinetic isotope effect for the uncatalysed reaction is in fair agreement with the results shown by other workers; the C¹⁴ effect is a little higher than predictable from literature evidence. The theoretical values for k_{12}/k_{13} and k_{12}/k_{14} on the basis of the Bigeleisen theory are 1.044 and 1.083 respectively at 25°. The former value is in agreement with the C¹³ kinetic isotope effect for the uncatalysed reaction, but the latter fails to predict any of the C¹⁴ results. The similarity between the

results in each row for the complexes is ascribed to the similar nature of the metal ions in these complexes and gives no indication of any paramagnetic effect. This suggests that chemical parallelism between a paramagnetic effect due to nuclear spin and one due to unpaired (4f) electrons is absent. Previous work on this topic is therefore also in doubt (11). The difference between the kinetic isotope effect for the uncatalysed reaction and the corresponding effect for the complexes is attributed to the inductive effect of the metal ions.

Future Prospects.

On the theoretical side, no really satisfactory model for predicting kinetic isotope effects has been obtained (24), the one proposed by Bigeleisen being the most useful so far. The difficulty is that even if all the frequencies for the substrate could be evaluated for both "light" and "heavy" molecules, the problems of the transition state and the temperature independent factor still remain. This latter is being tackled in an ingenious manner by Yankwich and co-workers (see p.65). Further, the standard equation itself (p.63, eqn. (xi)) is not entirely free from criticism, due to the approximations in its derivation, and more especially with regard to the ignoring of the tunnel effects and cancellation of the transmission coefficients in the application of the equation to chemical systems by Bigeleisen et al.

Some attempt was made by Bigeleisen (24) to allow for tunnel effects and to tackle the mass problem in calculating the temperature independent factor, but the resulting equation was more complex and not much more satisfactory than the currently accepted one.

From the experimental point of view, there are also many problems. It would be desirable to examine temperature effects for C¹³ and C¹⁴, for oxaloacetic acid, working at 50°, say, in order to obtain a significant difference in kinetic isotope effect. By performing experiments at various pHs, the assumption (see p.54) that oxaloacetic acid and its monoanion have the same kinetic isotope effect could be verified. The effect of varying the ionic charge of the complexing cation or trying substituted oxaloacetic acids could be investigated. The inductive effect question might also be approached via infra-red work on suitable compounds with a view to determining the best bond frequencies to be used in the theoretical calculations. Looking farther afield, isotope effects for elements other than carbon (preferably lighter ones, in order to increase the effect of small mass differences) might be studied if suitable systems are available. A large field of absorbing work lies before both theoretician and experimentalist, a field which may contain fundamental and vital new evidence on some of the profounder aspects of chemical kinetics.

APPENDICES.

Appendix A : Errors in the Determination of Kinetic Isotope Effects.

The expression given by Bigeleisen and Allen (12) can be derived as follows.

Consider, e.g., the equation,

$$k_2/k_1 = \ln(1 - f \cdot N_x/N_{x^0})/\ln(1 - f).$$

where k_1 refers to the "light" reaction. For convenience, put $k_2/k_1 = k$ and $N_x/N_{x^0} = N$. All terms have their usual meanings (p.7).

$$\therefore k = \ln(1 - fN)/\ln(1 - f).$$

$$\therefore k - 1 = \frac{\ln(1 - fN)}{\ln(1 - f)} - 1 = \frac{\ln(1 - fN)/(1 - f)}{\ln(1 - f)}$$

$$(k - 1)\ln(1 - f) = \ln \frac{1 - f + f - fN}{1 - f} = \ln \left[1 + \frac{f(1 - N)}{(1 - f)} \right]$$

Consider $(k - 1)$, f and $(1 - N)$ as variables : $(k - 1)$ is a function of both f and $(1 - N)$. Take derivatives of both sides of the above equation.

$$\therefore \delta(k - 1)\ln(1 - f) - \frac{(k - 1)\delta f}{(1 - f)}$$

$$= \frac{1}{1 + \frac{f(1 - N)}{(1 - f)}} \times \frac{(1 - f)[\delta f(1 - N) + f\delta(1 - N)] + f(1 - N)\delta f}{(1 - f)^2}$$

On dividing the above equation throughout by $(k - 1) \cdot \ln(1 - f)$, rearranging, and noting the expression for $(k - 1) \cdot \ln(1 - f)$ given on p.81, it can readily be shown that,

$$\frac{\delta(k - 1)}{(k - 1)} = \frac{[f/(1 - f)]\delta(1 - N) + (1 - N)[\delta f/(1 - f)^2]}{\left(1 + \frac{f(1 - N)}{(1 - f)}\right) \cdot \ln\left(1 + \frac{f(1 - N)}{(1 - f)}\right)} + \frac{\delta f}{(1 - f)\ln(1 - f)}$$

There is an additional factor in the denominator of the first term on the right hand side, as compared to Bigeleisen and Allen's original equation (12), as already pointed out by Tong and Yankwich (22). Insertion of suitable values for N , f , N and f shows that the error, as measured by the left hand side of the above equation, increases with increasing f , slowly at first and then very rapidly over 80% reaction, as the difference between N_x and N_{x0} becomes very small.

Appendix B. N_x^0/N_x values for graph of Fig.1. See p.9.

KIE = Kinetic Isotope effect. Table 13.

KIE	f	5	10	15	20	25	50	75	85	95	100
1.00		1	1	1	1	1	1	1	1	1	1
1.02	1.0195	1.0190	1.0184	1.0179	1.0173	1.0139	1.0093	1.0067	1.0032	1	
1.04	1.0390	1.0379	1.0368	1.0357	1.0345	1.0278	1.0186	1.0135	1.0065	1	
1.06	1.0585	1.0569	1.0553	1.0536	1.0518	1.0417	1.0280	1.0204	1.0098	1	
1.08	1.0780	1.0759	1.0737	1.0714	1.0691	1.0556	1.0374	1.0274	1.0153	1	
1.10	1.0975	1.0948	1.0921	1.0898	1.0864	1.0695	1.0469	1.0344	1.0168	1	
1.12	1.1169	1.1138	1.1105	1.1072	1.1036	1.0835	1.0564	1.0414	1.0205	1	
1.14	1.1364	1.1328	1.1290	1.1250	1.1209	1.0975	1.0659	1.0485	1.0240	1	
1.16	1.1559	1.1517	1.1474	1.1429	1.1382	1.1115	1.0755	1.0557	1.0277	1	
1.18	1.1754	1.1707	1.1658	1.1608	1.1555	1.1255	1.0852	1.0630	1.0514	1	
1.20	1.1949	1.1897	1.1843	1.1786	1.1728	1.1596	1.0949	1.0702	1.0353	1	

Appendix C : Preparation of C¹³-enriched Oxaloacetic Acid.

(See p.18).

7½% enrichment allowed for. By calculation, 5.98 gm of barium carbonate were required to supply the carbon dioxide for the Grignard reagent.

$$\text{Atomic weight of } 7\frac{1}{2}\%-C^{13} \text{ carbon} = \frac{12 \times 92.5 + 13 \times 7.5}{100} \\ = 12.075.$$

$$\therefore 197.4 \text{ gm (1 mole) BaC}^{13}O_3 \text{ contains } 0.975 \text{ gm C}^{13} (7\frac{1}{2}\%). \\ 5.98 " " " 0.975 \times 5.98/197.4 \text{ gm C}^{13}. \\ = 0.0295 \text{ gm C}^{13}.$$

(The dash denotes enriched carbon).

197.4 gm of ordinary barium carbonate contain 0.143 gm C¹³ (1.1%); 20.30 gm of the enriched carbonate supplied contain 1 gm C¹³.

Let x gm be the weight of enriched carbonate required and y gm the weight of ordinary carbonate.

$$\therefore x + y = 5.98 \text{ gm} \dots \dots \dots \text{(i)}$$

Also x gm enriched material contain $x/20.30$ gm C¹³ and y gm ordinary material contain $0.143y/197.4$ gm C¹³.

$$\therefore x/20.30 + 0.143y/197.4 = 0.0295 \dots \dots \text{(ii)}$$

Etc. Solution of (i) and (ii) gives x = 0.52 gm and y = 5.46 gms.

Appendix D : Preparation of Geiger-Counter Cathodes.

After polishing carefully with emery paper then Brasso, the cathode is "passivated" by treatment with the following solutions.

Solution A : 300 gm. NH_4Cl ,

90 ml. concentrated HCl,

50 ml. 0.2% (by weight) gelatine solution.

Make up to 1 litre with water.

Solution B : 250 gm. chromic acid,

75 ml. sulphuric acid,

35 ml. of solution A,

50 ml. of the gelatine solution.

Make up to 1 litre with water.

Solution C : 250 gm. chromic acid,

75 ml. sulphuric acid.

Make up to 1 litre with water.

- Procedure : (a) Place the copper or brass object in solution A and leave until all the oxide has dissolved, or for not more than 8 minutes. The solution should be at 80° .
- (b) Treat with solution B at 25° for not more than 2 minutes.
- (c) Wash with water.
- (d) Treat with solution C for a few seconds to reoxidise object, rewash, rinse with alcohol and leave to dry. Normally A is unnecessary.

Appendix E : Cl¹⁴ Content of Radioactive Oxaloacetic Acid.

(See pp. 39 and 45).

Cl¹⁴ decays to N¹⁴ with the emission of an electron (an β -particle). The half life of the process is given variously as between 5,000 and 6,000 years (see, e.g., 67). 0.5 millicuries (in a very small quantity of sodium acetate) were supplied.

Therefore the activity was $0.5 \times 10^{-3} \times 3.7 \times 10^{10}$ or 1.85×10^7 disintegrations per second, since 1 curie is 3.7×10^{10} disintegrations per second.

Applying the usual first order equation we have,

$$kt_{\frac{1}{2}} = 2.303 \cdot \log_{10} 2$$

where k is the rate constant and $t_{\frac{1}{2}}$ the half-life.

\therefore here,

$$k = \frac{2.303 \times \log 2}{6,000 \times 365 \times 24 \times 60 \times 60} = 3.66 \times 10^{-12} \text{ sec}^{-1}$$

Also by the first order law, $dc/dt = kc = \text{rate of production of particles.}$

$$\therefore 1.85 \times 10^7 = 3.66 \times 10^{-12} \times c.$$

$$\begin{aligned}\therefore c &= \text{number of unstable nuclei in original sample} \\ &= 1.85 \times 10^7 / 3.66 \times 10^{-12} \\ &= 5.055 \times 10^{18}\end{aligned}$$

Therefore the ratio of the number of unstable nuclei in the sodium acetate (or oxaloacetic acid) to the total number of nuclei is given by,

$$\frac{5.055 \times 10^{18}}{6.023 \times 10^{23} \times 18.6/82.04} = 3.70 \times 10^{-5},$$

where 6.023×10^{23} is the Avogadro number, 18.6 gm is the weight of sodium acetate used and 82.04 is its molecular weight.

Hence the concentration of C¹⁴ is negligible (about 4 atoms in 100,000).

Appendix F : Demonstration Verification of the Teller-Redlich Theorem for a Diatomic Molecule (see p.61).

Equation (v) on p.61 can be expressed, for a diatomic molecule, in the form,

$$\left(\frac{I_2}{I_1}\right) \cdot \left(\frac{M_2}{M_1}\right)^{3/2} \cdot \left(\frac{m_1}{m_2}\right)^{3/2} \cdot \left(\frac{\nu_1}{\nu_2}\right),$$

taking the left hand side and remembering the molecule still has two (equal) moments of inertia.

If the molecule can be represented as masses m_1 (or m_2) and m_3 connected by a spring of length l and stiffness k , where m_1 and m_2 are the isotopic masses and k is the bond force constant, we have, from simple dynamics,

$$I_1 = \frac{m_1 m_3 l^2}{m_1 + m_3} \quad \text{and} \quad I_2 = \frac{m_2 m_3 l^2}{m_2 + m_3}.$$

Also if the frequencies ν are in cycles per second (i.e., sec^{-1}),

$$\nu_1 = \frac{1}{2\pi} \sqrt{\frac{k(m_1 + m_3)}{m_1 \cdot m_3}} \quad \text{and} \quad \nu_2 = \frac{1}{2\pi} \sqrt{\frac{k(m_2 + m_3)}{m_2 \cdot m_3}}$$

$$\text{Finally, } M_1 = m_1 + m_3 \quad \text{and} \quad M_2 = m_2 + m_3.$$

On insertion of these values for I , ν and M into the initial expression, all the terms are found to cancel, leaving unity, which verifies the Theorem.

Appendix G : Proof of the Equation (viii), p.62.

We have (equation (vii)),

$$f \cdot \frac{s_2}{s_1} = \prod_{i=1}^{3n-6} \frac{u_i}{u_i + \Delta u_i} \cdot e^{\Delta u_i/2} \cdot \frac{(1 - e^{-(u_i + \Delta u_i)})}{(1 - e^{-u_i})}.$$

On taking logs (to the base e) of both sides of this equation, changing the sign on both sides, and noting that $\ln(fs_2/s_1) \doteq fs_2/s_1 - 1$, when f is significant, and also that $\ln(1 + \Delta u_i/u_i) \doteq \Delta u_i/u_i$, when Δu_i is small, we find,

$$\begin{aligned} & -(fs_2/s_1 - 1) \\ &= \sum \left(-\Delta u_i/2 + \Delta u_i/u_i + \ln(1 - e^{-u_i}) - \ln(1 - e^{-u_i} + \Delta u_i \cdot e^{-u_i}) \right) \\ &= -\sum \left(\Delta u_i (1/2 - 1/u_i) + \ln(1 + \Delta u_i \cdot e^{-u_i}/(1 - e^{-u_i})) \right) \\ &= -\sum \left(\Delta u_i (1/2 - 1/u_i) + \Delta u_i \cdot e^{-u_i}/(1 - e^{-u_i}) \right), \end{aligned}$$

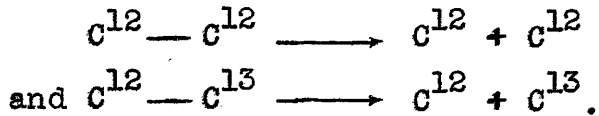
expanding the log in the second last line. Note that the range of summation has been omitted temporarily, to simplify the presentation.

$$\therefore s_2 f / s_1 = 1 + \sum_{i=1}^{3n-6} (1/2 - 1/u_i - 1/(e^{u_i} - 1)) \cdot u_i ,$$

which is equation (viii).

Appendix H : Calculation of the Temperature Independent Factor in C¹³-Kinetic Isotope Effect Bond Fission for Ethane (see p.65).

We have, following Slater (60),



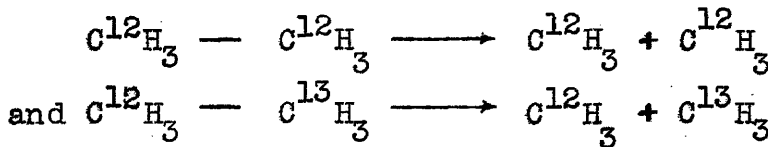
The reduced masses are, respectively,

$$\mu_1 = \frac{12 \times 12}{12 + 12} \quad \text{and} \quad \mu_2 = \frac{12 \times 13}{12 + 13}$$

$$= 6.000 \quad = 6.240.$$

∴ The temperature independent factor is $\left(\frac{6.240}{6.00}\right)^{\frac{1}{2}}$
 $= 1.01980.$

Note that if we treat the fission on the molecular-fragment theory (see p.64 and ref. 24) we have,



∴ the reduced masses are, respectively,

$$\mu_1 = \frac{15 \times 15}{15 + 15} \quad \text{and} \quad \mu_2 = \frac{15 \times 16}{15 + 16}$$

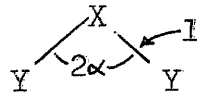
$$= 7.500 \quad = 7.742.$$

∴ the temperature independent factor is $\left(\frac{7.742}{7.500}\right)^{\frac{1}{2}} = 1.01601$,

a lower value than before.

Appendix I : Calculation of the Shift in Vibrational Frequencies for the Change in Constituent Masses between 45-14-45 and 46-14-46. (See p.68).

The appropriate formulae are given by Herzberg (62; p.169) and the force constants by Bigeleisen (68) from Herzberg. The model is XY_2 ,



There are three vibrational frequencies, given by,

$$\lambda_1 + \lambda_2 = 4\pi^2(\nu_1^2 + \nu_2^2) = (1 + \frac{2m_y}{m_x} \cos^2 \alpha) \frac{k_1}{m_y} + \frac{2}{m_y} (1 + \frac{2m_y}{m_x} \sin^2 \alpha) \frac{k_6}{l^2}$$

$$\lambda_1 \lambda_2 = 16\pi^4 \nu_1^2 \nu_2^2 = 2(1 + \frac{2m_y}{m_x}) \cdot \frac{k_1}{m_y^2} \cdot \frac{k_6}{l^2}$$

$$\text{and } \lambda_3 = 4\pi^2 \nu_3^2 = (1 + \frac{2m_y}{m_x} \sin^2 \alpha) \cdot k_1 / m_y.$$

The ms are the masses of the atoms, α and l are as shown and the ks are force constants. The ν 's are in sec^{-1} .

(a) Starting with the last equation and representing the square of the frequency for the heavy molecule by c, we have, dividing the "C¹²" equation by the "C¹³" one,

$$\nu_3^2/c = \frac{46(1 + 45(\sin^2 \alpha)/7)}{45(1 + 46(\sin^2 \alpha)/7)}$$

Putting $\alpha = 54^\circ 44'$, we find $c = 0.996 \times \nu_3^2$, and giving ν_3 a value of 905 cm^{-1} , $\sqrt{c} = 903 \text{ cm}^{-1}$.

(b) Representing the squares of the frequencies for the 46-14-46 molecule by a and b for convenience, inserting the appropriate masses and taking the second equation first, we have, dividing the "heavy" equation by the "light" one,

$$\frac{ab}{(\nu_1 \nu_2)^2} = \frac{(1 + 46/7)}{(1 + 45/7)} \cdot \left(\frac{45}{46} \right)^2$$

where the ν 's refer to the C^{12} (i.e., 45-14-45) molecule.

Putting $\nu_1 = 756 \text{ cm}^{-1}$ and $\nu_2 = 230 \text{ cm}^{-1}$ (see ref. 68), we have,

$$ab = (230 \times 756)^2 \times 0.9754 = 2.9490.$$

(Strictly, the ν 's are in sec^{-1} , but the factor correcting cm^{-1} to sec^{-1} cancels).

From the first equation, we have (68), similarly,

$$\frac{a + b}{\nu_1^2 + \nu_2^2} = \frac{\frac{4.1}{46} + (2 \times 4.1 \times \cos^2 54^\circ 44')/14 + (2 \times 0.35)/46 + (4 \times 0.35 \times \sin^2 54^\circ 44')/14}{\frac{4.1}{45} + (2 \times 4.1 \times \cos^2 54^\circ 44')/14 + (2 \times 0.35)/45 + (4 \times 0.35 \times \sin^2 54^\circ 44')/14}$$

On inserting $\alpha = 54^\circ 44'$, $\nu_1 = 756$ and $\nu_2 = 230$, we find,

$$a + b = 6.205 \times 10^5$$

These two equations are easily solved, giving a and

b and thence \sqrt{a} and \sqrt{b} .

Hence for the shift from 45-14-45 to 46-14-46,
we have the following frequency data. (The ws refer to
the observed frequencies).

	w_c^{12}	w_c^{13}
w_1	756 cm^{-1}	754 cm^{-1}
w_2	230 "	228 "
w_3	905 "	903 "

Appendix J: Demonstration Calculation of a C¹⁴-Kinetic Isotope Effect on Pitzer's Model (see p.73).

$T = 100^{\circ}\text{C}$; $u = 3.8547 \times 10^{-3} w$, inserting the values for the constants in the equation $u = hcw/kT$ (see p.61). The $G(u)$ terms were obtained from Bigeleisen & Mayer's paper (57). We have, using Pitzer's frequency data (51),

Table 14.

w ₁₂	u ₁₂	w ₁₄	u ₁₄	u	G(u ₁₄)	G(u ₁₄)	u
NORMAL MOLECULE							
1800	6.939	1713	6.603	0.336	0.3499	0.1176	
837	3.226	834	3.215	0.011	0.2308	0.0025	
493	1.900	490	1.889	0.011	0.1488	0.0016	
1423	5.485	1346	5.188	0.297	0.3129	0.0929	
483	1.862	481	1.854	0.008	0.1463	0.0012	
700	2.698	659	2.540	0.158	0.1919	0.0303	
							0.2461
ACTIVATED COMPLEX							
1711	6.595	1633	6.295	0.300	0.3430	0.1029	
1088	4.194	1053	4.059	0.135	0.2712	0.0366	
							0.1395

$$\therefore \text{KIE} = \text{TIF} \times \text{TDF}$$

$$\begin{aligned}
 &= (\text{reduced mass factor}) \times (\text{vibration factor}), \\
 &= 1.03775 (1 + 0.2461 - 0.1395) \\
 &= \underline{\underline{1.1484}}.
 \end{aligned}$$

References.

1. Urey and Grief, J.A.C.S., 57, 321, 1935.
2. Gelles and Nancollas, Trans. Far. Soc., 52, 98, 1956.
3. Gelles and Salama, J.C.S., 3683, 1958.
4. Pitzer and Gelles, J.A.C.S., 75, 5132, 1953.
5. Gelles and Pitzer, ibid., 77, 1974, 1955.
6. Gelles, ibid., 75, 6199, 1953.
7. Gelles, Nature, 176, 925, 1955.
8. Gelles and Clayton, Trans. Far. Soc., 52, 353, 1956.
9. Gelles, J.C.S., 4736, 1956.
10. Gelles and Hay, ibid., 3673, 1958.
11. Gelles and Reed, Nature, 176, 1262, 1955.
12. Bigeleisen and Allen, J. Chem. Phys., 19, 760, 1951.
13. Bothner-By and Bigeleisen, ibid., 19, 755, 1951.
14. Collins and Lietze, J.A.C.S., 81, 5379, 1959.
15. Melander, Arkiv. Kemi, 2, 211, 1950.
16. Hay, "The Catalysed Decarboxylation of Oxaloacetic Acid", PhD. Dissertation, (Glasgow), 1959.
17. Yankwich et al., "Isotopic Carbon"
18. Gilman, Zoellner and Dickey, J.A.C.S., 51, 1576, 1929.
19. Rossi and Schintz, Helv. Chim. Acta, 31, 473, 1948.
20. Wislicenus, Ann., 246, 317, 1888.
21. Mitz, Axelrod and Hofman, J.A.C.S., 72, 1231, 1950.
22. Tong and Yankwich, J. Phys. Chem., 61, 540, 1957.
23. Pedersen, Acta Chem. Scand., 6, 243, 1952.

24. Bigeleisen and Wolfsberg, Adv. Chem. Phys., 1, 15, 1958.
25. Bigeleisen and Friedman, J. Chem. Phys., 17, 998, 1949.
26. Lindsay, Bourns and Thode, Can. J. Chem., 30, 163, 1952.
27. Yankwich, Belford and Fraenkel, J.A.C.S., 75, 832, 1953.
28. Stevens, Pepper and Lounsbury, J. Chem. Phys., 20, 192, 1952.
29. Yankwich and Ikeda, J.A.C.S., 81, 5054, 1959.
30. Riesz and Bigeleisen, ibid., 81, 6187, 1959.
31. Seltzer, Hamilton and Westheimer, ibid., 81, 4018, 1959.
32. Lindsay, Bourns and Thode, Can. J. Chem., 29, 192, 1951.
33. Yankwich and Belford, J.A.C.S., 75, 4178, 1953.
34. Benson, J. Chem. Phys., 20, 1064, 1952.
35. Glascock, "Isotopic Gas Analysis for Biochemists".
36. Ropp and Raaen, J.A.C.S., 74, 4992, 1952.
37. Yankwich, Promislow and Nystrom, J.A.C.S., 76, 5893, 1954.
38. Yankwich and Weber, ibid., 27, 4513, 1955.
39. Roe and Albenesius, ibid., 74, 2402, 1952.
40. Stevens and Crowder, Can J. Chem., 32, 792, 1954.
41. Ropp, Bonner, Clark and Raaen, J.A.C.S., 76, 1710, 1954.
42. Ropp, J. Chem. Phys., 23, 2196, 1955.
43. Bonner and Tanner, J.A.C.S., 80, 1447, 1958.
44. Yankwich and Stivers, J. Chem. Phys., 21, 61, 1953.
45. Yankwich and Promislow, J.A.C.S., 76, 4648, 1954.
46. Yankwich, Stivers and Nystrom, J. Chem. Phys., 20, 344, 1952.
47. Yankwich and Belford, J.A.C.S., 76, 3067, 1954.

48. Yankwich and Weber, J.A.C.S., 78, 564, 1956.
49. Yankwich and Ikeda, ibid., 82, 1891, 1960.
50. Yankwich and Calvin, J. Chem. Phys., 17, 109, 1949.
51. Pitzer, ibid., 17, 1341, 1949.
52. Roe and Hellman, ibid., 19, 660, 1951.
53. Fry and Calvin, J. Phys. Chem., 56, 901, 1952.
54. Grigg, Austral. J. Chem., 2, 252, 1956.
55. Glasstone, Laidler and Eyring, "The Theory of Rate Processes".
56. Bigeleisen, J. Chem. Phys., 17, 675, 1949.
57. Bigeleisen and Mayer, ibid., 15, 261, 1947.
58. See ref. 24.
59. Wolfsberg, J. Chem. Phys., 33, 21, 1960.
60. Slater, Proc. Roy. Soc., 194 A, 112, 1948.
61. Bigeleisen, J. Phys. Chem., 56, 823, 1952.
62. Herzberg, "Infrared and Raman Spectra".
63. Glasstone, "Textbook of Physical Chemistry".
64. Bigeleisen and Wolfsberg, J. Chem. Phys., 21, 2120, 1953.
65. Kohlrausch, "Der Smekel-Raman Effekt".
66. Moeller, "Inorganic Chemistry. An Advanced Textbook".
67. Hawkings, Hunter, Mann and Stevens, Can. J. Chem., 27, 545, 1949.
68. Bigeleisen, J. Chem. Phys., 17, 425, 1949.
69. Fieser, "Experiments in Organic Chemistry".
70. Vogel, "Practical Organic Chemistry".